

26. X-RAY MINERALOGY STUDIES—LEG 11¹

I. Zemmels and H. E. Cook, University of California, Riverside, California,
and
J. C. Hathaway, U. S. Geological Survey, Woods Hole, Massachusetts

PART 1 (I. Zemmels and H. E. Cook)

Introduction

Semiquantitative determinations of the mineral composition in bulk samples and the <2-micrometer² fraction, and qualitative determinations in the 2 to 20-micrometer fraction of Leg 11 sediments were performed by H. E. Cook and I. Zemmels according to the methods described in the reports of Legs 1 and 2 and in Appendix III of Volume IV. The mineral analyses of the 2 to 20-micrometer and <2-micrometer fractions were performed on calcite-free residues. The results are presented in Tables 1 through 10 and in Figures 1 through 24. A suite of special samples was analyzed separately by J. C. Hathaway and is described later in this chapter.

No semiquantitative determinations of the mineral concentrations were made for the silt fractions (2 to 20 micrometers). Instead, selected minerals which commonly have an authigenic origin were sought and are reported in Tables 1 through 10 on a ranked scale. The minerals sought were: barite, phillipsite, clinoptilolite, erionite, dolomite, siderite, rhodochrosite, goethite, hematite, magnetite, cristobalite, pyrite, and apatite. The minerals were ranked according to an approximate semiquantitative scale as follows: major (M) > 25 per cent, abundant (A) 25 to 8 per cent, present (P) 8 to 2 per cent and trace (T) <2 per cent. The values of the diffuse scattering, amorphous scattering, and the two most abundant minerals are also included to help characterize the sample.

Drilling mud was used on Leg 11 as follows: gel mud (a montmorillonite bentonite) was used in drilling Cores 14 and 15 in Hole 98, Cores 4 to 15 in Hole 99A; gel mud was used after drilling to fill Hole 100 and 101A, gel mud with barite was used to fill Holes 102 and 103.

No barite was detected in the sediments from Holes 102, 103 or subsequent holes. Montmorillonite contamination was not positively detected. An abrupt

increase in the montmorillonite content of the <2-micrometer fraction in Cores 8 to 11 in Hole 99 coincides with a change in lithology as well as the use of drilling mud. No sample of the drilling mud was available for comparison.

Montmorillonites with two types of expansion behavior were encountered in the samples from Leg 11. The normal expansion to 18Å with trihexylamine acetate was observed in most cases. In some samples, however, montmorillonite which expanded to only 14Å was found. The nonexpanding montmorillonite occurred in pure form as well as in mixtures with normally-expanding montmorillonite. No errors were found in the laboratory procedures, and the nonexpanding montmorillonites could be made to expand normally after a brief autoclave treatment. It was found that the height of the peak at 14Å in the nonexpanded form nearly equaled the height of the peak at 18Å in the fully-expanded form after autoclaving. Therefore, the semiquantitative estimate of montmorillonite based on nonexpanded forms is considered to be relatively accurate.

The type of montmorillonite used in the estimate is designated in Tables 1 to 10 as follows:

A percentage with no other designation means that the estimate was made from a sample of normally-expanding montmorillonite.

A superscript (a) is used to indicate that the estimate was made from a 14Å form of montmorillonite. A correction for the 14Å chlorite peak was applied wherever necessary.

A superscript (b) indicates that the determination was made on the sum of both 14Å and 18Å peaks.

The X-ray mineralogy results are discussed in the framework of lithologic units established by the shipboard scientists of Leg 11 and by Lancelot *et al.* (this volume). No samples from Site 107 were submitted for X-ray analyses.

RESULTS

Site 98

Hole 98 was drilled in Northeast Providence Channel, a deep embayment northeast of Andros Island, with the

¹Contribution No. 2772 of the Woods Hole Oceanographic Institution.

²The 13th General Conference on Weights and Measures, Paris, 1967, adopted the unit micrometer (μm) in place of the former unit "micron" (μ).

TABLE 1 – Continued

Hole 98: 2-20 μ m

Core	Depth	Sample Depth Below Sea Floor (m)	Diff.	% Amorph.	Major Constituent						
					1	2	Dolo.	Cris.	Clin.	Pyri.	Bari.
1	0-9	0.78-2.33	65.4	46.0	Mica	Quar.	A				
		3.76-4.34	64.8	45.0	Mica	Dolo.	A				
		5.03-5.52	65.7	46.3	Mica	Quar.					
		6.23-6.72	63.8	43.4	Mica	Quar.	P				
		7.80-8.31	65.6	46.3	Mica	Quar.					
2	9-18	9.39-12.62	60.6	38.4	Mica	Quar.				T	
		13.66-17.43	77.9	65.5	Mica	Quar.	T		T	T	
3	18-27	18.33-26.13	68.5	50.8	Mica	Quar.			T	T	
		22.25-22.27	68.2	50.3	Mica	Quar.			T	A	
4	55-64	55.12-63.19	68.0	49.9	Mica	Quar.			T	P	
5	93-102	93.73-98.23	87.1	79.9	Mica	Quar.			P		
6	130-139	130.17-133.95	88.6	82.2	Mica	Quar.					
		134.63-138.32	88.3	81.7	Mica	Quar.			A		
7	167-176	167.16-175.15	68.7	51.2	Cris.	Clin.		N	A		P
8	207-216	207.39-210.69	96.5	94.6	Mica	Quar.					
9	216-222	216.86-218.26	94.3	91.0	Mica	Quar.					P
10	222-231	222.74-223.47	72.7	57.3	Cris.	Quar.		N	A		
11	231-240	232.31-233.75	55.2	30.0	Clin.	Mica			N		
12	240-241	240.25-240.67	59.3	36.4	Mica	Clin.			N		

TABLE 1 – Continued

Hole 98: <2 μm

Core	Depth	Sample Depth Below Sea Floor (m)	Diff.	%			Cris.	Arag.	Plag.	Kaol.	Mica	Chlo.	Mont.	Paly.	Clin.	Pyri.	Gyps.
				Amorph.	Quar.												
1	0-9	0.34-0.34	86.1	78.3	14.5	—	—	4.1	14.6	45.9	7.0	14.1	—	—	—	—	—
		0.78-2.33	81.9	71.8	8.5	—	—	1.6	5.4	38.5	6.5	39.6	—	—	—	—	—
		3.76-4.34	82.4	72.5	5.5	—	—	—	14.9	22.9	3.3	52.3	—	—	—	—	1.1
		5.03-5.52	83.7	74.5	6.1	—	—	—	10.5	30.7	7.9	44.8 ^a	—	—	—	—	—
		6.23-6.72	80.5	69.6	10.6	—	—	1.6	10.2	40.6	5.6	31.5	—	—	—	—	—
		7.80-8.31	79.5	68.0	10.6	—	—	—	—	27.9	7.3	54.1	—	—	—	—	—
2	9-18	9.39-12.62	81.3	70.8	10.3	—	—	—	11.2	23.8	6.5	46.4 ^a	—	—	—	—	1.8
		13.66-17.40	80.4	69.4	10.1	—	—	—	13.8	27.9	3.3	44.9 ^a	—	—	—	—	—
3	18-27	18.33-26.13	80.9	70.2	7.0	—	—	—	17.8	24.5	1.8	48.9	—	—	—	—	—
		22.26-22.26	83.5	74.3	7.3	—	—	—	23.0	27.0	3.9	35.3 ^b	—	—	—	—	—
4	55-64	55.12-63.19	78.0	65.7	7.9	—	—	—	8.4	19.9	5.4	57.3 ^a	—	—	—	—	1.2
5	93-102	93.73-98.23	78.5	66.4	13.2	—	—	—	13.3	28.9	2.2	15.0 ^a	24.1	3.3	—	—	—
6	130-139	130.17-133.95	80.8	70.0	3.9	—	—	—	29.0	15.2	—	51.9	—	—	—	—	—
		134.63-138.32	81.8	71.4	3.7	—	—	—	17.4	14.3	—	52.1	10.4	2.1	—	—	—
7	167-176	167.16-175.15	82.1	72.1	2.4	19.1	—	—	—	9.8	—	52.3	9.8	5.3	—	—	1.4
8	207-216	207.39-210.69	87.7	80.8	3.1	—	—	—	15.4	14.2	—	53.2	14.0	—	—	—	—
9	216-222	216.86-218.26	87.3	80.2	4.4	—	—	—	13.6	15.6	—	55.4	11.0	—	—	—	—
10	222-231	222.74-223.47	86.5	78.9	11.2	22.2	—	—	—	9.5	—	41.8	7.0	8.4	—	—	—
11	231-240	232.31-233.75	88.2	81.6	7.8	—	—	—	—	—	—	58.8	16.0	14.3	—	—	3.0
12	240-241	240.25-240.67	84.3	75.5	6.9	—	—	—	—	17.7	2.3	63.6	9.4	—	—	—	—
13	272-281	273.39-274.52	89.4	83.5	3.8	—	—	—	1.5	14.1	—	24.7	55.9	—	—	—	—
14	311-318	311.66-312.20	89.2	83.2	6.8	—	—	—	—	31.0	2.6	35.4	24.2	—	—	—	—
15	348-357	349.07-349.07	84.8	76.2	7.0	—	—	—	—	25.2	2.7	34.8	31.2	—	—	—	—

^aIndicates that the estimate was made from a 14Å form of montmorillonite. A correction for the 14Å chlorite peak was applied wherever necessary.

^bIndicates that the determination was made on the sum of both 14Å and 18Å peaks.

TABLE 2
Results of X-Ray Diffraction Analysis from Site 99

Hole 99A: Bulk

Core	Depth	Sample Depth Below Sea Floor (m)	Diff.	% Amorph.	Calc.	Dolo.	Quar.	Cris.	K-Fe.	Plag.	Kaol.	Mica	Chlo.	Mont.	Amph.
1	0-9	0.40-6.76	71.5	55.4	36.0	2.9	17.7	—	7.0	6.7	2.8	22.5	2.1	0.0	2.1
2	15-21	15.00-21.00	74.1	59.5	35.8	11.5	17.6	—	—	3.3	3.6	22.6	2.1	3.4	—
8	94-100	95.03-95.44	54.8	29.4	97.1	—	1.1	—	—	—	—	1.8	—	—	—
9	131-140	132.04-132.17	47.5	18.0	97.1	—	0.5	2.4	—	—	—	—	—	—	—
11	198-202	199.12-199.12	47.7	18.3	98.6	—	1.4	—	—	—	—	—	—	—	—

Hole 99A: 2-20 μ m

Core	Depth	Sample Depth Below Sea Floor (m)	Diff.	% Amorph.	Major Constituent					
					1	2	Cris.	Clin.	Pyri.	
1	0-9	0.40-6.76	69.1	51.7	Mica	Quar.			T	
2	15-21	15.00-21.00	69.2	51.8	Mica	Quar.				
8	94-100	95.03-95.44	72.5	57.0	Mica	Cris.	M	P	T	
9	131-140	132.04-132.17	71.8	56.0	Mica	Cris.	M	T	T	
11	198-202	199.12	65.5	46.1	Quar.	Mica			P	

Hole 99A: <2 μ m

Core	Depth	Sample Depth Below Sea Floor (m)	Diff.	% Amorph.	Quar.	Cris.	Plag.	Kaol.	Mica	Chlo.	Mont.	Paly.
1	0-9	0.40-6.76	69.1	51.7	12.0	—	3.8	5.2	39.0	6.9	21.5 ^b	11.6
2	15-21	15.00-21.00	69.2	51.8	13.4	—	—	12.9	37.2	3.6	23.7 ^b	9.1
8	94-100	95.03-95.44	72.5	57.0	10.5	11.1	—	2.0	25.5	—	50.9 ^a	—
9	131-140	132.04-132.17	71.8	56.0	4.6	49.1	—	—	—	—	46.2 ^a	—
11	198-202	199.12-199.12	65.5	46.1	31.5	—	—	—	16.5	—	52.0	—

^aIndicates that the estimate was made from a 14Å form of montmorillonite. A correction for the 14Å chlorite peak was applied wherever necessary.

^bIndicates that the determination was made on the sum of both 14Å and 18Å peaks.

TABLE 3
Results of X-Ray Diffraction Analysis from Site 100

Hole 100: Bulk

Core	Depth	Sample Depth Below Sea Floor (m)	Diff.	% Amorph.	Calc.	Quar.	K-Fe	Plag.	Mica	Chlo.	Paly.
1	203-212	204.20-209.69	47.3	17.7	97.3	2.7	—	—	0.0	—	—
		205.61-205.61	53.2	26.9	91.0	4.6	—	—	4.4	—	—
2	237-246	240.74-240.74	58.0	34.3	83.3	6.3	—	—	6.1	—	4.3
3	246-259	247.50-247.65	48.7	19.9	52.5	47.5	—	—	0.0	—	—
4	259-261	259.31-259.31	66.2	47.1	59.6	12.7	—	1.0	19.2	1.0	6.5
		259.66-259.66	64.2	44.1	60.4	12.6	—	2.5	24.5	—	—
5	261-267	262.81-262.81	74.7	60.5	45.0	16.4	—	—	18.0	0.6	20.0
6	267-276	267.23-267.23	70.2	53.4	52.3	14.3	—	1.6	19.0	1.2	11.7
		268.31-268.31	66.0	46.8	72.0	8.6	—	—	10.4	1.1	7.9
7	276-286	276.45-276.45	48.1	18.9	98.1	0.8	—	—	0.0	1.1	—
		277.05-278.87	62.7	41.7	94.1	5.9	—	—	0.0	—	—
8	286-292	287.40-290.50	61.6	40.0	91.1	3.0	1.8	—	4.1	—	—
9	302-311	302.75-304.25	66.4	47.4	86.5	3.3	4.7	—	5.4	—	—
10	311-317	311.68-313.34	68.6	51.0	83.0	5.4	3.9	—	6.5	1.1	—

Hole 100: 2-20 μ m

Core	Depth	Sample Depth Below Sea Floor (m)	Diff.	% Amorph.	Major Constituents		Bari.	Pyri.	Paly.
					1	2			
1	203-212	204.20-209.69	55.2	30.0	Quar.	Mica			
		205.63	65.5	46.1	Mica	Quar.			
2	237-246	240.74	63.8	43.5	Mica	Quar.			
3	246-259	247.50-247.65	48.1	18.8	Quar.	—			
4	259-261	259.31	68.6	50.9	Mica	Quar.			P
		259.66	66.4	47.4	Mica	Quar.			
5	261-267	262.81	69.0	51.5	Mica	Quar.			P

TABLE 3 – Continued

Core	Depth	Sample Depth Below Sea Floor (m)	Diff.	% Amorph.	Major Constituents					
					1	2	Bari.	Pyri.	Paly.	
6	267-276	267.23	63.0	42.1	Mica	Quar.				T
		268.31	62.5	41.4	Mica	Quar.				
7	276-286	276.45	67.3	49.0	Mica	Quar.	A			
		277.05-278.87	65.0	45.3	Mica	Quar.				
8	286-292	287.40-290.50	65.0	45.3	Mica	Quar.			T	
9	302-311	302.75-304.25	73.3	58.3	Mica	K-Fe			T	T
10	311-317	311.68-313.34	65.9	46.7	Quar.	Mica				

Hole 100: <2 μ m

Core	Depth	Sample Depth Below Sea Floor (m)	Diff.	% Amorph.	Major Constituents								
					Quar.	Kaol.	Mica	Chlo.	Mont.	Paly.	Hema.	Gyps.	K-Fe
1	203-212	204.20-209.69	82.0	71.9	40.6	–	17.2	–	25.6	16.6	–	–	–
		205.61-205.61	83.4	74.0	49.0	–	30.6	2.4	2.9	15.1	–	–	–
2	237-246	240.74-240.74	85.3	77.0	39.0	–	31.1	–	6.1	23.8	–	–	–
3	246-259	247.50-247.65	48.7	19.8	94.3	–	2.8	–	–	2.9	–	–	–
4	259-261	259.31-259.31	88.0	81.0	18.7	–	35.0	4.0	2.9	35.8	3.6	–	–
		259.66-259.66	82.2	72.1	17.9	–	38.2	2.8	–	41.1	–	–	–
5	261-267	262.81-262.81	83.6	74.4	17.6	–	–	2.4	17.4	62.6	–	–	–
6	267-276	267.23-267.23	85.5	77.4	12.9	–	37.7	1.6	–	47.8	–	–	–
		268.31-268.31	87.4	80.3	10.6	–	15.9	–	9.7 ^b	63.8	–	–	–
7	276-286	276.45-276.45	82.8	73.2	28.5	–	21.5	1.1	39.6	9.3	–	–	–
		277.05-278.87	80.4	69.3	20.2	2.8	16.2	–	42.0 ^a	18.7	–	–	–
8	286-292	287.40-290.50	91.7	87.0	6.3	–	25.1	5.7	30.3	32.5	–	–	–
9	302-311	302.75-304.25	86.5	78.9	14.8	3.6	–	–	80.1 ^a	–	–	1.5	–
10	311-317	311.68-313.34	91.9	87.3	18.3	–	26.0	2.9	13.3 ^b	26.8	–	–	12.4

^aIndicates that the estimate was made from a 14A form of montmorillonite. A correction for the 14A chlorite peak was applied wherever necessary.

^bIndicates that the determination was made on the sum of both 14A and 18A peaks.

TABLE 4
Results of X-Ray Diffraction Analysis from Site 101

Hole 101: Bulk

Core	Depth	Sample Depth Below Sea Floor (m)	Diff.	% Amorph.	Calc.	Dolo.	Quar.	K-Fe	Plag.	Kaol.	Mica	Chlo.	Mont.	Pyri.
1	32-41	32.20-40.92	73.3	58.2	15.0	2.1	22.8	—	5.2	6.7	37.0	2.9	8.4 ^a	—
2	67-76	68.46-74.37	73.5	58.5	11.8	11.0	31.8	7.4	10.5	7.7	3.4	1.7	12.3 ^a	2.4

Hole 101: 2-20 μ m

Core	Depth	Sample Depth Below Sea Floor (m)	Diff.	% Amorph.	Major Constituent			
					1	2	Clin.	Pyri.
1	32-41	32.20-40.91	65.3	45.7	Mica	Quar.	T	T
2	67-76	68.46-74.37	63.8	43.5	Mica	Quar.	T	T

Hole 101: <2 μ m

Core	Depth	Sample Depth Below Sea Floor (m)	Diff.	% Amorph.	Quar.	Kaol.	Mica	Chlo.	Mont.
1	32-41	32.20-40.92	80.2	69.0	11.6	8.6	25.8	5.2	48.8 ^a
2	67-76	68.46-74.37	82.2	72.2	12.5	14.5	27.5	2.6	42.9

Hole 101A: Bulk

Core	Depth	Sample Depth Below Sea Floor (m)	Diff.	% Amorph.	Calc.	Dolo.	Arag.	Side.	Quar.	K-Fe	Plag.	Kaol.	Mica	Chlo.	Mont.	Pyri.
1	115-124	116.00-119.02	75.4	61.5	5.0	2.9	—	2.1	34.5	8.2	9.6	8.6	5.3	3.8	14.9	5.3
2	156-165	156.41-164.50	74.7	60.5	15.9	5.0	3.6	2.1	19.6	—	5.5	9.2	23.6	1.6	7.7	6.1
3	194-203	195.20-196.92	74.8	60.6	5.5	13.2	—	1.2	28.0	4.8	4.7	5.0	28.4	2.3	5.0	1.9
4	250-259	250.38-251.22	74.6	60.3	—	—	—	—	19.6	—	3.4	6.1	43.3	3.4	24.2 ^a	—
5	308-317	308.25-310.30	80.1	68.9	8.8	—	—	—	20.2	—	11.7	1.6	42.2	1.6	13.8 ^a	—
6	380-389	380.58-380.60	72.2	56.6	—	—	—	—	21.8	—	6.0	2.8	58.7	4.2	6.4 ^b	—
		380.70-380.72	73.6	58.8	—	—	—	—	20.8	—	4.7	3.3	62.7	3.6	4.9 ^a	—

TABLE 4 – Continued

Core	Depth	Sample Depth Below Sea Floor (m)	Diff.	% Amorph.	Calc.	Dolo.	Arag.	Side.	Quar.	K-Fe	Plag.	Kaol.	Mica	Chlo.	Mont.	Pyri.
		381.26-381.28	76.8	63.8	–	–	–	–	22.6	–	5.6	–	67.5	4.3	–	–
7	460-469	460.98-461.22	71.3	55.1	–	–	–	–	24.6	6.2	6.7	–	37.7	1.6	23.2 ^a	–
8	534-543	534.56-534.58	72.7	57.4	–	24.8	–	19.2	17.1	–	3.8	2.6	3.0	–	29.6 ^a	–
		534.98-536.40	74.0	59.3	–	–	–	–	29.2	–	5.7	–	37.1	2.2	25.8 ^a	–
9	599-610	599.44-600.23	52.6	26.0	95.6	–	–	–	2.3	–	–	–	2.1	–	–	–
10	685-691	685.78-686.30	51.4	24.1	93.3	1.2	–	–	3.7	–	–	–	1.8	–	–	–

Hole 101A: 2-20 μ m

Core	Depth	Sample Depth Below Sea Floor (m)	Diff.	% Amorph.	Major Constituent		Pyri.
					1	2	
1	115-124	116.00-119.02	65.8	46.5	Mica	Quar.	P
2	156-165	156.41-164.50	68.4	50.6	Mica	Quar.	T
3	194-203	194.20-196.92	69.5	52.3	Mica	Quar.	P
4	250-259	250.38-251.22	69.6	52.6	Mica	Quar.	
5	308-317	308.25-310.30	73.0	57.8	Mica	Quar.	T
6	380-389	380.59	73.1	58.0	Mica	Quar.	
		380.71	61.7	40.1	Mica	Quar.	
		381.27	63.9	43.7	Mica	Quar.	
7	460-469	460.98-461.22	61.7	40.2	Mica	Quar.	
8	534-543	534.57	69.6	52.6	Mica	Quar.	T
		534.98-536.40	71.5	55.4	Mica	Quar.	T
9	599-610	499.44-600.23	70.3	53.6	Mica	Quar.	P
10	685-691	685.78-686.30	65.3	45.7	Quar.	Mica	P

TABLE 4 –Continued

Hole 101A: < 2 μm

Core	Depth	Sample Depth Below Sea Floor (m)	Diff.	% Amorph.	Quar.	Plag.	Kaol.	Mica	Chlo.	Mont.	Hema.
1	115-124	116.00-119.02	84.2	75.3	10.1	—	16.2	31.1	—	42.6	—
2	156-165	156.41-164.50	80.5	69.6	5.8	—	13.2	21.1	2.0	57.8	—
3	195-203	195.20-196.92	83.1	73.6	5.9	—	15.6	18.5	—	60.0	—
4	250-259	250.38-251.22	77.4	64.7	1.9	—	10.0	9.4	—	78.6	—
5	308-317	308.25-310.30	75.6	61.9	9.6	2.0	—	42.3	1.7	44.4	—
6	380-389	380.59-380.59	90.4	85.0	13.9	—	10.1	64.7	3.4	7.9	—
		380.71-380.71	92.1	87.6	12.8	—	14.3	64.6	3.3	5.0	—
		381.27-381.27	87.2	80.0	12.4	—	11.1	45.3	—	31.2	—
7	460-469	460.98-461.22	77.4	64.7	12.5	—	—	24.1	—	63.4	—
8	534-543	534.57-534.57	79.5	68.0	10.7	—	—	28.8	1.4	55.4	3.6
		534.98-536.40	81.0	70.3	21.7	—	—	20.3	—	58.0	—
9	599-610	599.44-600.23	81.5	71.1	36.9	—	—	18.0	—	45.1	—
10	685-691	685.78-686.30	81.3	70.8	64.3	—	—	22.8	1.9	11.0	—

^aIndicates that the estimate was made from a 14Å form of montmorillonite. A correction for the 14Å chlorite peak was applied wherever necessary.

^bIndicates that the determination was made on the sum of both 14Å and 18Å peaks.

TABLE 5
Results of X-Ray Diffraction Analysis from Site 102

Hole 102: Bulk

Core	Depth	Sample Depth Below Sea Floor (m)	Diff.	% Amorph.												
				Calc.	Dolo.	Side.	Quar.	K-Fe	Plag.	Kaol.	Mica	Chlo.	Mont.	Paly.	Amph.	
1	0-9	0.43-8.76	71.8	55.9	12.2	2.3	—	20.8	—	7.9	6.1	44.8	5.9	—	—	—
2	18-27	19.24-25.95	74.0	59.4	8.3	2.7	—	23.0	—	14.5	2.2	41.1	6.2	—	—	2.0
3	58-67	59.40-59.92	73.5	58.6	20.5	3.1	—	21.9	—	8.6	5.5	35.4	3.4	—	—	1.6
4	96-105	97.25-101.76	70.9	54.5	22.6	2.6	—	20.1	—	6.6	4.3	39.3	4.4	—	—	—
5	133-142	133.03-141.77	71.5	55.4	24.3	3.8	—	21.2	—	16.5	1.5	26.3	3.9	—	—	2.4
6	172-181	172.44-180.76	72.5	57.0	29.4	4.5	—	18.0	6.1	11.6	2.9	25.2	2.4	—	—	—
7	181-191	181.40-189.80	74.4	60.1	21.5	4.9	—	21.3	—	13.4	3.4	29.2	3.8	—	—	2.5
8	219-228	220.24-226.98	76.0	62.6	17.3	2.8	—	22.9	—	14.9	3.4	31.6	3.1	1.8	—	2.1
9	266-275	266.43-274.76	73.8	59.0	34.9	2.2	—	22.4	—	6.0	3.7	27.7	3.0	0.0	—	—
10	306-315	306.66-313.96	73.5	58.6	15.2	1.6	—	22.4	—	4.7	7.4	37.2	2.6	8.9 ^a	—	—
11	353-357	353.89-357.00	75.7	62.1	24.9	—	—	23.8	—	5.1	2.6	29.3	2.9	11.3 ^b	—	—
12	419-423	419.27-423.00	74.0	59.4	24.7	—	—	20.7	3.7	4.4	5.0	32.8	2.7	6.0 ^a	—	—
13	473-476	473.43-476.00	74.3	59.9	18.3	—	—	23.5	2.2	6.3	4.9	31.6	2.2	11.0 ^a	—	—
14	512-513	512.00-513.00	74.8	60.7	24.4	—	1.3	20.6	1.7	3.9	2.8	25.9	2.7	11.1 ^a	5.7	—
15	548-549	548.57-549.00	75.5	61.8	29.0	—	—	21.9	2.6	3.1	5.8	27.7	1.3	8.6 ^b	—	—
16	584-585	584.21-584.21	77.2	64.4	14.7	2.7	—	27.7	—	5.7	9.5	26.9	—	12.9 ^b	—	—
17	618-619	618.44-619.00	74.7	60.4	17.4	—	—	24.7	2.2	5.7	7.5	25.3	—	17.1 ^a	—	—
18	634-636	634.00-636.00	72.2	56.6	18.9	—	—	26.1	—	5.1	8.1	28.1	—	13.7 ^a	—	—
19	659-661	659.42-660.28	76.0	62.5	17.5	—	—	22.7	4.4	4.8	10.7	23.4	1.5	12.9 ^a	—	2.1

Hole 102: 2-20 μm

Core	Depth	Sample Depth Below Sea Floor (m)	Diff.	% Amorph.	Major Constituents			
					1	2	Clin.	Pyri.
1	0-9	0.43-8.76	61.4	39.7	Mica	Quar.		
2	18-27	19.24-25.95	61.6	39.9	Mica	Quar.		

TABLE 5 – Continued

Core	Depth	Sample Depth Below Sea Floor (m)	Diff.	%	Major Constituents			
					Amorph.	1	2	Clin.
3	58-67	59.40-59.92	64.4	44.4	Mica	Quar.		
4	96-105	97.25-101.76	61.8	40.3	Mica	Quar.		
5	133-142	133.03-141.77	63.9	43.6	Mica	Quar.		
6	172-181	172.44-180.76	64.1	44.0	Mica	Quar.		
7	181-191	181.40-189.80	66.2	47.1	Mica	Quar.		T
8	219-228	220.24-226.98	66.4	47.4	Mica	Quar.		T
9	266-275	266.43-274.76	63.6	43.1	Mica	Quar.		T
10	306-315	306.66-319.96	66.2	47.2	Mica	Quar.		P
11	353-357	353.89-357.00	69.7	52.7	Mica	Quar.	T	T
12	419-423	419.27-423.00	66.8	48.1	Mica	Quar.	T	T
13	473-476	473.43-476.00	67.3	48.9	Mica	Quar.	T	T
14	512-513	512.00-513.00	66.8	48.1	Mica	Quar.	T	T
15	548-549	548.57-549.00	67.6	49.4	Mica	Quar.	T	T
16	584-585	584.21	not available		Mica	Quar.		T
17	618-619	618.44-619.00	53.0	26.6	Quar.	Mica		T
18	634-636	634.00-636.00	66.1	47.0	Mica	Quar.	T	T
19	659-661	659.42-660.28	62.8	41.9	Mica	Quar.	T	P

Hole 102: <2 μ m

Core	Depth	Sample Depth Below Sea Floor (m)	Diff.	%							
					Amorph.	Quar.	Plag.	Kaol.	Mica	Chlo.	Mont.
1	0-9	0.43-8.76	80.9	70.1	12.9	3.6	9.1	57.4	6.5	10.4	–
2	18-27	19.24-25.95	85.1	76.7	14.0	10.8	2.2	49.4	8.6	13.0	1.9
3	58-67	59.40-59.92	82.4	72.5	13.7	5.0	7.9	42.6	8.0	22.9	–
4	96-105	97.25-101.76	84.9	76.4	15.4	4.9	11.7	48.7	3.9	15.5	–
5	133-142	133.03-141.77	82.5	72.6	17.0	16.7	3.5	44.2	7.3	8.2	3.0
6	171-181	172.44-180.76	84.4	75.6	14.6	8.9	3.9	42.9	5.7	24.1	–

TABLE 5 – Continued

Core	Depth	Sample Depth Below Sea Floor (m)	Diff.	% Amorph.	Quar.	Plag.	Kaol.	Mica	Chlo.	Mont.	Amph.
7	181-191	181.40-189.80	85.0	76.6	15.6	11.3	6.3	39.1	5.4	20.8	1.5
8	219-228	220.24-226.98	85.5	77.3	14.5	8.2	8.9	36.9	2.9	26.5	2.1
9	266-275	266.43-274.76	84.8	76.3	15.9	3.1	11.6	41.8	2.4	25.2	–
10	306-315	306.66-313.96	82.7	72.9	10.0	–	18.4	27.7	–	43.9 ^a	–
11	353-357	353.89-357.00	80.8	70.0	9.6	–	12.8	27.4	–	50.3 ^a	–
12	419-423	419.27-423.00	78.1	65.8	10.3	1.6	13.0	24.7	3.0	47.5 ^a	–
13	473-476	473.43-476.00	77.1	64.3	8.3	–	14.6	23.5	–	53.6 ^a	–
19	659-661	659.42-660.28	82.0	71.9	18.0	1.5	18.9	31.1	2.5	28.0	–

^aIndicates that the estimate was made from a 14Å form of montmorillonite. A correction for the 14Å chlorite peak was applied wherever necessary.

^bIndicates that the determination was made on the sum of both 14Å and 18Å peaks.

TABLE 6
Results of X-Ray Diffraction Analysis from Site 103

Hole 103: Bulk

Core	Depth	Sample Depth Below Sea Floor (m)	Diff.	Amorph.	Calc.	Dolo.	Quar.	K-Fe	Plag.	Kaol.	Mica	Chlo.	Mont.	Pyri.
1	0-9	0.43-2.76	72.9	57.6	26.2	–	31.4	4.9	7.9	1.8	24.9	2.9	–	–
		3.47-4.96	73.2	58.1	22.1	1.6	30.9	–	6.2	5.2	27.6	1.5	2.8	2.1
		5.74-7.96	75.0	61.0	24.0	–	29.2	1.7	4.9	5.3	27.9	1.7	3.4	1.9
		8.78-8.80	74.0	59.4	26.4	–	34.2	–	8.3	3.0	22.8	2.1	3.2	–
2	39-48	39.29-47.76	75.1	61.1	16.1	8.2	20.9	–	10.5	8.9	28.0	–	7.6 ^a	–
3	94-103	95.95-98.26	74.7	60.5	0.0	–	31.0	1.8	7.8	6.2	37.3	2.1	13.8 ^a	–
		98.94-102.76	79.2	67.4	1.3	–	31.6	2.0	6.2	6.7	38.6	2.2	11.3 ^b	–
4	170-179	170.44-177.22	76.7	63.6	4.6	–	33.3	–	7.7	5.8	36.9	2.2	7.5 ^b	1.9
5	247-256	248.24-251.30	75.5	61.7	30.7	–	21.4	1.6	4.0	7.1	25.9	1.8	7.4 ^b	–
6	343-352	343.44-344.26	78.9	67.1	7.1	–	30.3	–	3.4	10.7	34.2	12.3	2.0 ^b	–

TABLE 6 – Continued

Hole 103: 2-20 μ m

Core	Depth	Sample Depth Below Sea Floor (m)	Diff.	Amorph.	Major Constituent			
					1	2	Clin.	Pyri.
1	0-8	0.43-2.76	60.6	38.5	Mica	Quar.		T
		3.47-4.96	60.7	38.6	Mica	Quar.	T	T
		5.47-7.96	62.1	40.8	Mica	Quar.		P
2	39-48	39.29-47.76	64.0	43.8	Mica	Quar.	T	P
3	94-103	95.95-98.26	63.3	42.6	Mica	Quar.	T	P
		98.94-102.76	66.2	47.1	Mica	Quar.		P
4	170-179	170.44-177.22	65.8	46.5	Mica	Quar.		T
5	247-256	248.24-251.30	63.5	42.9	Mica	Quar.		T
6	343-352	363.44-364.26	73.4	58.4	Mica	Quar.		P

Hole 103: <2 μ m

Core	Depth	Sample Depth Below Sea Floor (m)	Diff.	% Amorph.							
					Quar.	Kaol.	Mica	Chlo.	Mont.	Pyri.	Gyps.
1	0-8	0.43-2.76	81.9	71.8	10.5	15.5	31.9	—	40.8	—	1.3
		3.47-4.96	81.7	71.3	10.2	9.1	31.3	4.4	45.1	—	—
		5.74-7.96	80.7	69.9	9.0	6.9	22.4	4.8	56.9	—	—
2	39-48	39.29-47.76	84.6	75.9	12.7	16.9	27.1	—	41.4	1.9	—
3	94-103	95.95-98.26	80.5	69.6	9.9	11.4	27.4	2.3	49.0	—	—
		98.94-102.76	85.2	76.9	13.5	20.1	27.9	—	38.6	—	—
4	170-179	170.44-177.22	84.6	75.9	11.4	16.7	27.7	—	44.2	—	—
5	247-256	248.24-251.30	81.5	71.1	8.6	21.1	24.1	—	46.2	—	—
6	343-352	343.44-344.26	83.8	74.7	12.7	22.2	26.9	—	38.2	—	—

^aIndicates that the estimate was made from a 14Å form of montmorillonite. A correction for the 14Å chlorite peak was applied wherever necessary.

^bIndicates that the determination was made on the sum of both 14Å and 18Å peaks.

TABLE 7
Results of X-Ray Diffraction Analysis from Site 104

Hole 104: Bulk

Core	Depth	Sample Depth Below Sea Floor (m)	Diff.	% Amorph.	Calc.	Dolo.	Side.	Quar.	K-Fe	Plag.	Kaol.	Mica	Chlo.	Mont.	Paly.	Pyri.
1	0-9	0.44-3.46	75.1	61.0	8.3	—	—	31.5	8.1	8.8	6.4	30.3	—	6.6	—	—
		4.45-4.95	73.3	58.2	29.6	—	—	24.7	4.2	7.5	2.7	22.2	3.3	5.9	—	—
		5.74-8.76	75.5	61.7	—	—	—	36.6	3.3	8.5	9.0	31.3	—	8.4	—	2.8
2	36-45	36.70-44.76	75.4	61.6	16.4	—	—	24.6	—	2.9	9.8	38.0	—	4.3	—	4.0
3	62-71	62.44-70.76	80.9	70.1	9.4	—	—	33.3	4.9	4.9	10.3	27.6	—	5.9	—	3.6
4	133-142	134.30-141.18	79.9	68.6	2.9	—	—	30.9	—	6.5	10.2	36.2	—	11.1	—	2.2
6	219-228	219.68-227.88	81.8	71.5	14.4	—	2.6	24.2	—	2.2	13.0	29.1	—	8.0	4.8	1.6
7	306-315	306.32-311.76	80.5	69.5	22.1	1.4	—	23.0	—	4.5	8.7	24.9	—	5.5	8.4	1.5
8	401-410	402.30-408.32	79.1	67.3	29.3	—	—	22.2	—	1.8	10.0	24.1	—	4.6	6.1	1.9
9	495-504	495.50-499.25	81.7	71.3	23.3	—	3.8	21.8	—	2.9	9.8	29.9	—	7.2	—	1.4
10	615-617	615.90-615.92	80.2	69.1	23.0	2.7	—	20.0	—	1.1	2.8	27.5	—	10.1	11.0	1.8

Hole 104: 2-20 μ m

Core	Depth	Sample Depth Below Sea Floor (m)	Diff.	% Amorph.	Major Constituent		Clin.	Pyri.	Cris.
					1	2			
1	0-9	0.44-3.46	64.3	44.2	Quar.	Mica		T	
		4.45-4.95	63.3	42.7	Quar.	Mica		P	
		5.74-8.76	61.1	39.2	Quar.	Mica		P	
2	36-45	36.70-44.76	64.4	44.4	Mica	Quar.	T	P	
3	62-71	62.44-70.76	74.1	59.6	Mica	Quar.		P	
4	133-142	134.30-141.18	69.2	51.9	Mica	Quar.		T	
6	219-228	219.68-227.88	78.8	66.9	Mica	Quar.		P	P
7	306-315	306.32-311.76	76.1	62.7	Mica	Quar.		P	
8	401-410	402.31	77.9	65.5	Mica	Quar.		P	
9	495-504	495.50-499.25	81.6	71.2	Mica	Quar.		P	
10	615-617	615.91	77.0	64.1	Mica	Quar.		P	

TABLE 7 – Continued

Hole 104: < 2 μm

Core	Depth	Sample Depth Below Sea Floor (m)	Diff.	% Amorph.								Gyps.
				Quar.	Kaol.	Mica	Chlo.	Mont.	Paly.	Gyps.		
1	0-9	0.44-3.46	82.4	72.6	9.6	9.4	28.3	4.2	48.5	—	—	
		4.45-4.95	84.5	75.7	8.6	14.2	24.7	3.3	47.8	—	1.4	
		5.74-8.76	86.7	79.2	16.9	20.2	30.3	—	32.6	—	—	
2	36-45	36.70-44.76	85.1	76.7	14.0	25.4	28.6	—	32.0 ^b	—	—	
3	62-71	62.44-70.76	88.6	82.2	14.1	23.6	26.6	—	35.6 ^b	—	—	
4	133-142	134.30-141.18	87.6	80.6	13.6	20.3	33.2	—	32.8	—	—	
6	219-228	219.68-227.88	85.1	76.7	11.2	25.4	27.2	—	36.2 ^a	—	—	
7	306-315	306.32-311.76	88.2	81.5	12.9	19.8	26.4	—	31.4 ^a	9.5	—	
8	401-410	402.31-402.31	87.0	79.8	13.4	24.5	26.2	—	27.6 ^a	8.4	—	
9	495-504	495.50-499.25	84.0	75.1	9.5	20.5	25.8	—	44.2 ^a	—	—	
10	615-617	615.91-615.91	87.6	80.6	6.0	17.1	19.5	—	26.9 ^b	30.4	—	

^aIndicates that the estimate was made from a 14Å form of montmorillonite. A correction for the 14Å chlorite peak was applied wherever necessary.

^bIndicates that the determination was made on the sum of both 14Å and 18Å peaks.

TABLE 8
Results of X-Ray Diffraction Analysis From Site 105

Hole 105: Bulk

Core	Depth	Sample Depth Below Sea Floor (m)	Diff.	% Amorph.													
				Calc.	Dolo.	Quar.	Cris.	K-Fe	Plag.	Kaol.	Mica	Chlo.	Mont.	Clin.	Pyri.	Amph.	
2	31-40	31.50-35.32	60.9	39.0	10.2	2.7	24.8	—	16.2	25.6	—	14.9	2.1	—	—	—	3.5
3	91-100	91.44-96.76	72.5	57.0	13.1	—	24.5	—	—	7.1	4.6	38.0	3.7	9.0 ^a	—	—	—
4	184-193	184.44-192.76	72.5	57.0	—	—	26.4	—	4.3	5.7	5.6	40.7	3.8	13.5 ^a	—	—	—
5	241-250	242.24-245.22	78.3	66.1	—	—	17.5	—	—	7.5	7.6	28.5	—	4.6 ^a	34.3	—	—
6	250-259	250.78-252.76	77.5	64.8	—	—	23.4	—	4.8	3.4	9.2	52.8	—	6.4 ^b	—	—	—
7	259-268	259.82-267.72	79.8	68.4	—	—	33.6	—	5.0	4.8	8.1	48.6	—	—	—	—	—
8	268-277	268.20-276.55	76.5	63.3	—	—	30.4	—	3.9	2.7	6.7	49.2	2.6	4.5 ^b	—	—	—

TABLE 8 – Continued

Core	Depth	Sample Depth Below Sea Floor (m)	Diff.	%			Quar.	Cris.	K-Fe	Plag.	Kaol.	Mica	Chlo.	Mont.	Clin.	Pyri.	Amph.
				Amorph.	Calc.	Dolo.											
9	286-295	286.44-289.71	81.6	71.3	—	—	20.7	—	6.2	—	11.6	54.7	—	6.7	—	—	—
		290.49-295.00	74.9	60.8	—	—	22.8	—	—	2.4	—	51.9	3.1	15.4 ^b	—	4.3	—
10	295-304	295.60-297.80	75.8	62.3	—	—	15.8	—	—	3.1	—	46.9	2.7	31.6	—	—	—
11	304-313	304.44-311.02	73.5	58.5	9.9	—	10.2	—	—	3.6	1.4	29.2	—	21.9	23.8	—	—
12	313-322	314.13-318.80	73.0	57.9	9.2	—	8.4	—	—	1.7	—	26.1	1.5	15.6	37.5	—	—
13	322-331	323.40-330.90	73.0	57.9	5.1	—	10.4	6.5	—	3.3	—	26.0	—	17.4 ^b	31.3	—	—
14	348-357	349.24-349.50	69.4	52.1	—	—	11.2	—	—	2.2	—	38.5	1.7	16.3 ^a	30.1	—	—
15	366-375	367.42-374.26	70.4	53.7	—	—	9.8	—	—	3.2	—	29.4	2.0	17.1 ^a	38.5	—	—
16	385-392	386.04-387.04	76.9	64.0	—	—	6.9	33.6	1.3	2.5	—	20.8	—	11.9	23.0	—	—
17	403-412	403.44-407.22	57.5	33.6	94.0	—	1.2	—	—	—	—	3.4	—	—	1.3	—	—
18	421-430	421.22-429.90	60.0	37.5	93.7	—	2.0	—	—	—	—	4.3	—	—	—	—	—
19	430-439	432.06-435.92	74.3	59.9	9.0	—	9.9	—	—	—	—	32.0	2.4	19.1	27.6	—	—
20	439-448	439.73-439.88	56.5	32.0	94.1	—	1.9	—	—	—	—	4.0	—	—	—	—	—
21	448-457	449.37-449.39	62.6	41.6	83.1	—	6.1	—	—	—	—	7.3	—	1.8	1.7	—	—
22	457-466	458.51-459.39	51.8	24.6	95.0	—	2.4	—	—	—	—	2.7	—	—	—	—	—
23	466-475	467.08-468.22	47.9	18.5	96.9	—	1.5	—	—	—	—	1.5	—	—	—	—	—
24	475-484	475.95-477.47	60.7	38.6	85.1	—	6.5	—	—	—	—	5.6	—	2.8	—	—	—
25	484-493	484.46-488.20	53.9	28.0	93.1	—	3.1	—	—	—	—	2.4	—	1.3	—	—	—
26	493-502	493.60-495.96	57.6	33.8	86.1	—	6.4	—	—	—	—	4.3	—	3.2	—	—	—
27	502-511	502.51-505.76	52.8	26.2	89.5	—	7.7	—	—	—	—	1.6	—	1.2	—	—	—
28	511-522	511.03-519.27	55.5	30.4	89.4	—	8.0	—	—	—	—	2.6	—	—	—	—	—
29	522-531	522.98-526.43	55.1	29.9	84.6	—	8.2	—	—	—	—	3.2	—	4.0	—	—	—
30	531-540	531.81-533.85	56.2	31.5	82.9	—	9.2	—	—	—	—	6.4	—	1.5	—	—	—
31	540-549	542.40-542.70	49.9	21.7	95.6	—	2.9	—	—	—	—	1.6	—	—	—	—	—
32	549-558	551.61-551.65	57.7	33.9	86.2	—	6.8	—	—	—	—	4.7	—	2.3	—	—	—
33	558-567	559.14-559.16	53.3	27.0	93.8	—	3.6	—	—	—	—	2.6	—	—	—	—	—
		559.30-565.48	64.2	44.1	73.8	—	12.1	—	—	1.6	—	11.2	—	1.3	—	—	—

TABLE 8 – Continued

Core	Depth	Sample Depth		Diff.	%		Quar.	Cris.	K-Fe	Plag.	Kaol.	Mica	Chlo.	Mont.	Clin.	Pyri.	Amph.	
		Below Sea Floor (m)			Amorph.	Calc.												
34	567-576	568.30-574.28		68.8	51.2	36.1	—	22.0	—	—	3.4	—	35.6	1.3	1.6	—	—	—
35	576-585	577.00-581.89		71.8	56.0	39.3	—	20.1	—	—	5.2	—	29.1	1.4	4.9	—	—	—
36	585-594	586.65-586.67		74.7	60.4	17.4	—	27.7	—	—	8.0	—	36.8	4.0	6.1	—	—	—
		587.74-589.00		70.8	54.4	51.0	—	15.4	—	3.3	4.1	—	24.6	1.6	—	—	—	—
37	594-603	594.19-601.92		72.0	56.3	36.3	—	21.1	—	—	5.4	—	35.4	1.8	—	—	—	—
38	603-612	605.03-611.04		71.2	55.0	25.2	—	30.9	—	—	7.2	—	35.3	1.4	—	—	—	—
39	612-621	612.06-614.76		71.4	55.3	24.1	—	31.1	—	—	4.8	—	38.2	1.8	—	—	—	—

Hole 105: 2-20 μ m

Core	Depth	Sample Depth		Diff.	Amorph.	Major Constituent		Cris.	Clin.	Pyri.
		Below Sea Floor (m)				1	2			
2	31-40	31.50-35.32		60.1	37.6	Mica	Quar.			
3	91-100	91.44-96.76		64.4	44.3	Mica	Quar.			
4	184-193	184.44-192.76		67.2	48.7	Mica	Quar.			
5	241-250	242.24-245.22		60.3	38.0	Clin.	Mica		M	
6	250-259	250.78-252.76		58.5	35.1	Mica	Quar.			
7	259-268	259.82-267.72		57.9	34.2	Mica	Quar.		T	
8	268-277	268.20-276.55		60.6	38.4	Mica	Quar.			
		286-295	286.44-289.71	61.6	40.1	Mica	Quar.			
9	286-295	290.49-295.00		61.9	40.5	Mica	Quar.		A	P
		295-304	295.60-297.80	62.2	41.0	Mica	Quar.			
11	304-313	304.44-311.02		61.9	40.4	Mica	Clin.		A	T
12	313-322	314.13-318.80		62.5	41.5	Mica	Clin.	A	M	T
13	322-331	323.40-330.90		64.6	44.7	Mica	Quar.	P	A	T
14	348-357	349.24-349.50		64.7	44.9	Mica	Quar.		A	
15	366-375	367.42-374.26		62.8	41.8	Mica	Clin.		A	T
16	385-392	386.04-387.04		66.6	47.8	Mica	Cris.	M	A	T
17	403-412	403.44-407.22		67.3	48.8	Mica	Clin.		A	P

TABLE 8 – *Continued*

Hole	Depth	Sample Depth Below Sea Floor (M)	Diff.	% Amorph.	Major Constituent		Cris.	Clin.	Pyri.
					1	2			
18	421-430	421.22-429.90	64.3	44.3	Mica	Quar.		A	P
19	430-439	432.06-435.92	70.6	54.0	Mica	Quar.	P	A	T
20	439-448	439.73-439.88	68.5	50.8	Mica	Quar.		P	P
21	448-457	449.37	69.6	52.6	Mica	Quar.		A	P
22	457-466	458.51-459.39	67.0	48.4	Mica	Quar.		A	P
23	466-475	467.08-468.22	65.1	45.4	Mica	Quar.		A	P
24	475-484	475.95-477.47	71.6	55.7	Mica	Quar.			P
25	484-493	484.46-488.20	68.6	51.0	Mica	Quar.			P
26	493-502	493.60-495.96	62.0	40.6	Quar.	Mica			P
27	502-511	502.51-505.76	67.6	49.4	Quar.	Mica			P
28	511-522	511.03-519.27	66.3	47.3	Quar.	Mica			
29	522-531	522.98-526.43	64.5	44.6	Mica	Quar.			T
30	531-540	531.81-533.85	65.7	46.4	Quar.	Mica			
31	540-549	542.40-542.70	65.9	46.6	Mica	Quar.		T	
32	549-558	551.61-551.65	62.9	42.0	Mica	Quar.			
33	558-567	559.15	69.0	51.6	Mica	Quar.			
		559.30-565.48	65.7	46.4	Mica	Quar.			
34	567-576	568.30-574.28	62.5	41.5	Mica	Quar.			
35	576-585	577.00-581.89	61.4	39.7	Mica	Quar.		T	
36	585-594	586.66	65.6	46.3	Mica	Quar.			
		587.74-589.00	63.1	42.3	Mica	Quar.			
37	594-603	594.19-601.92	65.0	45.3	Mica	Quar.			
38	603-612	605.03-611.04	60.9	38.9	Mica	Quar.			
39	612-621	612.06-614.76	63.4	42.8	Mica	Quar.			

TABLE 8 – Continued

Hole 105: <math>\lt; 2\mu\text{m}</math>

Core	Depth	Sample Depth Below Sea Floor (m)	Diff.	% Amorph.												
				Quar.	Cris.	K-Fe	Plag.	Kaol.	Mica	Chlo.	Mont.	Clin.	Hema.	Amph.	Gyps.	
2	31-40	31.50-35.32	86.4	78.8	15.3	–	–	17.4	–	36.9	6.5	22.4	–	–	1.6	–
3	91-100	91.44-96.76	84.5	75.8	12.2	–	–	–	14.6	32.5	–	40.7	–	–	–	–
4	184-193	184.44-192.76	80.6	69.7	8.1	–	–	–	8.9	25.1	2.4	55.5	–	–	–	–
5	241-250	242.24-245.22	87.0	79.7	9.0	–	–	–	12.0	25.7	–	43.1	10.2	–	–	–
6	250-259	250.78-252.76	84.4	75.7	7.4	–	–	–	24.9	28.5	–	39.2	–	–	–	–
7	259-268	259.82-267.72	82.0	72.0	5.1	–	–	–	23.7	27.6	–	43.6	–	–	–	–
8	268-277	268.20-276.55	82.3	72.4	10.8	–	–	–	16.9	40.4	5.9	26.0	–	–	–	–
9	286-295	286.44-289.71	81.4	70.9	4.6	–	–	–	18.0	26.3	–	51.1	–	–	–	–
		290.49-295.00	75.7	62.1	5.4	–	–	–	10.0	19.4	–	64.2	1.5	–	–	–
10	295-304	295.60-297.80	72.8	57.5	7.7	–	–	–	2.9	30.0	1.6	57.8	–	–	–	–
11	304-313	304.44-311.02	75.2	61.3	3.5	–	2.7	–	–	15.5	–	78.3	–	–	–	–
12	313-322	314.13-318.80	74.9	60.7	4.9	–	–	–	–	22.0	–	70.3	2.8	–	–	–
13	322-331	323.40-330.90	73.1	58.0	3.7	–	–	–	–	17.1	–	79.1	–	–	–	–
14	348-357	349.24-349.50	70.2	53.4	2.5	–	2.1	–	–	14.1	–	81.4	–	–	–	–
15	366-375	367.42-374.26	74.3	59.8	2.4	–	–	–	–	14.1	–	83.6	–	–	–	–
16	386-392	386.04-387.04	82.8	73.1	2.2	14.8	–	–	–	16.4	–	66.5	–	–	–	–
17	403-412	403.44-407.22	89.5	83.6	8.9	–	–	–	–	41.7	–	49.3	–	–	–	–
18	421-430	421.22-429.90	83.9	74.9	7.1	–	–	–	–	23.6	–	69.3	–	–	–	–
19	430-439	432.06-435.92	70.9	54.5	1.5	–	–	–	–	14.4	–	84.1	–	–	–	–
20	439-448	439.73-439.88	82.9	73.2	12.9	–	–	–	–	17.1	–	70.1	–	–	–	–
21	448-457	449.37-449.37	86.2	83.0	16.6	–	–	–	–	18.8	–	64.6	–	–	–	–
22	457-466	458.51-459.39	77.4	64.7	21.9	–	–	–	–	13.9	–	61.2	2.9	–	–	–
23	466-475	467.08-468.22	77.4	64.7	11.9	–	–	–	–	12.1	–	74.3	1.7	–	–	–
24	475-484	475.95-477.47	80.7	69.8	16.8	–	–	–	–	11.7	–	71.6	–	–	–	–
25	484-493	484.46-488.20	82.1	72.1	32.7	–	–	–	–	13.7	–	53.6 ^a	–	–	–	–
26	493-502	493.60-495.96	77.5	64.9	19.8	–	–	–	–	9.8	–	66.6	–	–	–	3.9
27	502-511	502.51-505.76	73.8	59.1	67.2	–	–	–	–	7.0	–	25.8 ^a	–	–	–	–

TABLE 8 – Continued

Core	Depth	Sample Depth	Diff.	%												
		Below Sea Floor (m)		Amorph.	Quar.	Cris.	K-Fe	Plag.	Kaol.	Mica	Chlo.	Mont.	Clin.	Hema.	Amph.	Gyps.
28	511-522	511.03-519.27	76.8	63.8	62.3	–	–	–	–	10.0	–	27.7	–	–	–	–
29	522-531	522.98-526.43	71.8	55.9	34.2	–	–	–	–	7.8	–	57.9	–	–	–	–
30	531-540	531.81-533.85	75.7	62.0	51.1	–	–	–	–	11.7	–	37.2 ^a	–	–	–	–
31	540-549	542.40-542.70	75.1	61.1	32.8	–	–	–	–	11.1	–	56.1	–	–	–	–
32	549-558	551.63-551.63	73.7	58.9	26.6	–	–	–	–	12.5	–	61.0	–	–	–	–
33	558-567	559.15-559.15	73.8	59.1	20.9	–	–	–	–	15.3	–	63.8	–	–	–	–
		559.30-565.48	86.3	78.6	47.5	–	–	–	–	30.1	–	19.4	–	2.9	–	–
34	567-576	568.30-574.28	84.3	75.5	41.8	–	–	–	–	28.8	–	29.4 ^b	–	–	–	–
35	576-585	577.00-581.89	91.1	86.1	26.8	–	–	–	–	54.1	–	16.1	–	3.0	–	–
36	585-594	586.66-586.66	89.7	83.9	22.7	–	–	–	–	53.0	–	24.3	–	–	–	–
		587.74-589.00	89.6	83.8	17.8	–	–	–	–	63.3	2.1	13.5	–	3.4	–	–
37	594-603	594.19-601.92	83.4	74.1	17.3	–	–	–	3.2	54.4	–	22.1 ^a	–	3.0	–	–
38	603-612	605.03-611.04	84.8	76.3	35.8	–	–	–	–	52.8	1.6	6.8 ^b	–	3.0	–	–
39	612-621	612.06-619.76	86.7	79.2	34.2	–	–	–	2.8	46.1	–	13.5	–	3.4	–	–

^aIndicates that the estimate was made from a 14Å form of montmorillonite. A correction for the 14Å chlorite peak was applied wherever necessary.

^bIndicates that the determination was made on the sum of both 14Å and 18Å peaks.

TABLE 9
Results of X-Ray Diffraction Analysis from Site 106

Hole 106: Bulk

Core	Depth	Sample Depth Below Sea Floor (m)	Diff.	% Amorph.	Calc.	Dolo.	Quar.	K-Fe	Plag.	Kaol.	Mica	Chlo.	Amph.
1	0-7	1.09-6.46	69.1	51.7	13.5	2.5	22.1	—	10.3	4.3	41.3	4.7	1.2
2	45-50	46.25-46.25	68.8	51.3	4.0	4.6	30.6	—	33.8	1.7	17.9	2.5	4.9
3	110-119	110.82-118.76	61.8	40.3	6.2	—	37.4	15.0	21.3	1.3	14.9	1.5	2.5
5	263-272	264.14-266.43	76.1	62.7	14.7	2.5	22.7	—	17.9	3.2	33.0	3.7	2.3

Hole 106: 2-20 μm

Core	Depth	Sample Depth Below Sea Floor (m)	Diff.	% Amorph.	Major Constituent		
					1	2	Pyri.
1	0-7	1.09-6.46	61.1	39.3	Mica	Quar.	
2	45-50	46.25	58.2	34.7	Quar.	Plag	T
3	110-119	110.82-118.76	68.9	51.4	Mica	Quar.	
5	263-272	264.14-266.43	66.2	47.1	Mica	Quar.	
6	340-349	340.44-343.44	64.9	45.2	Mica	Quar.	T

Hole 106: < 2 μm

Core	Depth	Sample Depth Below Sea Floor (m)	Diff.	% Amorph.	Quar.	Plag.	Kaol.	Mica	Chlo.	Mont.	Paly.	Amph.
1	0-7	1.09-6.46	81.1	70.5	15.5	4.8	8.4	55.6	5.2	10.6	—	—
2	45-50	46.25-46.25	86.8	79.3	13.4	15.3	4.9	37.8	7.2	18.1 ^b	—	3.4
3	110-119	110.82-118.76	83.9	74.8	10.2	2.7	6.3	51.7	4.9	23.3	—	—
5	263-272	264.14-266.43	86.3	78.6	13.4	15.0	—	44.8	4.7	21.0	—	—
6	340-349	340.44-343.44	93.2	89.4	13.6	6.6	—	45.4	6.5	17.9	9.9	—

^aIndicates that the estimate was made from a 14Å form of montmorillonite. A correction for the 14Å chlorite peak was applied wherever necessary.

^bIndicates that the determination was made on the sum of both 14Å and 18Å peaks.

TABLE 9 – Continued

Hole 106B: Bulk

Core	Depth	Sample Depth Below Sea Floor (m)	Diff.	% Amorph.										
				Calc.	Dolo.	Quar.	Cris.	Plag.	Kaol.	Mica	Chlo.	Mont.	Pyri.	
1	366-375	366.76-369.78	77.8	65.3	6.7	1.6	23.0	–	5.9	7.5	40.0	3.1	12.2 ^b	–
2	451-460	452.09-456.29	77.7	65.1	13.5	–	22.7	–	6.4	6.1	38.2	2.9	10.2 ^a	–
3	553-562	553.64-561.29	79.6	68.2	7.3	–	24.8	–	–	7.2	41.9	3.3	15.6 ^b	–
4	754-763	756.02-759.65	78.5	66.5	–	–	24.5	–	–	6.3	44.0	3.1	22.0	–
5	935-944	935.14-943.82	77.3	64.6	–	–	30.4	–	4.1	2.6	34.5	2.6	23.6	2.0
6	954-961	954.75-957.30	75.5	61.7	–	–	17.9	6.4	2.5	2.0	28.1	1.5	40.0	1.6
7	1012-1015	1012.36-1012.36	77.9	65.5	–	–	4.8	55.7	–	–	8.5	–	31.0	–

Hole 106B: 2-20 μ m

Core	Depth	Sample Depth Below Sea Floor (m)	Diff.	% Amorph.		Major Constituent		Cris.	Clin.	Pyri.
				1	2	1	2			
1	366-375	386.76-389.78	65.4	45.9	Mica	Quar.			T	T
2	451-460	452.09-456.29	66.3	47.3	Mica	Quar.			T	T
3	553-562	553.64-561.29	71.1	54.9	Mica	Quar.			T	T
4	754-763	756.02-759.65	70.9	54.5	Mica	Quar.			T	T
5	935-944	735.14-743.82	74.1	59.5	Mica	Quar.				P
6	954-961	954.75-957.30	72.7	57.3	Mica	Quar.				P
7	1012-1015	1012.36	76.4	63.1	Cris.	–		M		

TABLE 9 – continued

Hole 106B: <2 μ m

Core	Depth	Sample Depth Below Sea Floor (m)	Diff.	% Amorph.	Quar.	Kaol.	Mica	Chlo.	Mont.	Cris.
1	366-375	366.76-369.78	80.2	69.1	10.0	10.3	31.2	3.1	45.4	–
2	451-460	452.09-456.29	85.5	77.3	13.6	9.3	29.2	2.0	46.0	–
3	553-562	553.64-561.29	83.7	74.5	8.7	7.1	20.5	13.0	50.8	–
4	754-763	756.02-759.65	85.1	76.7	11.7	14.9	21.0	–	52.4	–
5	935-944	935.14-943.82	79.7	68.3	5.1	5.0	10.5	–	79.4	–
6	954-961	954.75-957.30	78.5	66.4	6.1	5.0	11.5	–	77.5	–
7	1012-1015	1012.36-1012.36	86.0	78.2	3.5	0.0	9.4	–	33.5	53.6

TABLE 10
Results of X-Ray Diffraction Analysis from Site 108

Hole 108: Bulk

Core	Depth	Sample Depth Below Sea Floor (m)	Diff.	% Amorph.	Calc.	Dolo.	Arag.	Quar.	K-Fe	Plag.	Kaol.	Mica	Chlo.	Mont.	Amph.
1	39-57	39.98-46.02	73.0	57.9	82.5	–	1.0	2.9	–	–	–	4.1	–	9.5	–
2	57-75	57.75-57.75	62.1	40.1	2.2	1.1	–	30.3	13.3	19.8	3.4	24.7	2.4	–	2.7

Hole 108: 2-20 μ m

Core	Depth	Sample Depth Below Sea Floor (m)	Diff.	% Amorph.	% Major Constituent	
					1	2
1	39-57	39.98-46.02	93.9	90.5	Quar.	Mica
2	57-75	57.75	57.3	33.3	Mica	Quar.

Hole 108: <2 μ m

Core	Depth	Sample Depth Below Sea Floor (m)	Diff.	% Amorph.	Quar.	Plag.	Kaol.	Mica	Chlo.	Mont.	Amph.
1	39-57	39.98-46.02	82.2	72.2	3.0	–	1.6	7.4	–	88.0	–
2	57-75	57.75-57.75	81.4	71.0	14.4	6.5	12.7	55.5	6.8	2.6	1.5

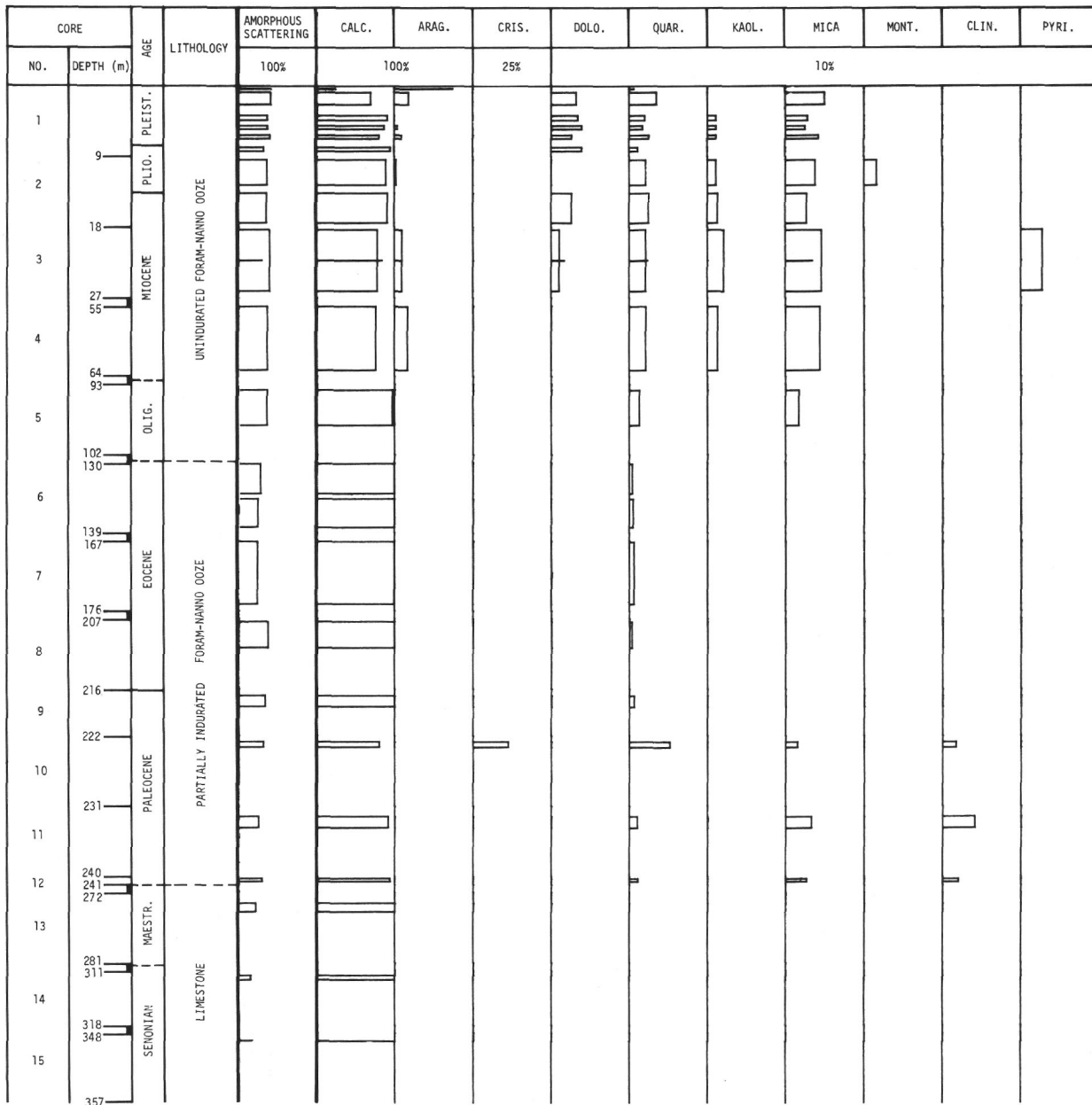


Figure 1. Hole 98, Bulk.

objective of studying the history and development of the Bahama Banks. Three lithologic units were recognized here by the shipboard scientists.

Upper Unit (Cores 1 – 5)

This unit consists of an unconsolidated foraminiferal-nannoplankton ooze, Holocene to Late Oligocene in age. Some pyroclastic materials were noted by the shipboard geologists in the Late Miocene sediments, but generally there is scarcity of allogenic matter, such as terrigenous debris or pollen. Mica, quartz and kaolinite are the only lithogenous minerals detected in

the bulk samples. Aragonite and dolomite occur frequently in the upper unit (Figure 1).

The major components of the decalcified 2 to 20-micrometer fraction are mica and quartz (Table 1). Dolomite occurs in the upper cores. Clinoptilolite, which occurs in the lower cores, may be stratigraphically associated with the volcanic detritus. Mica, montmorillonite and kaolinite make up the major proportion of the <2-micrometer fraction (Figure 2: Table 1). Chlorite occurs in small amounts and is restricted to the upper unit.

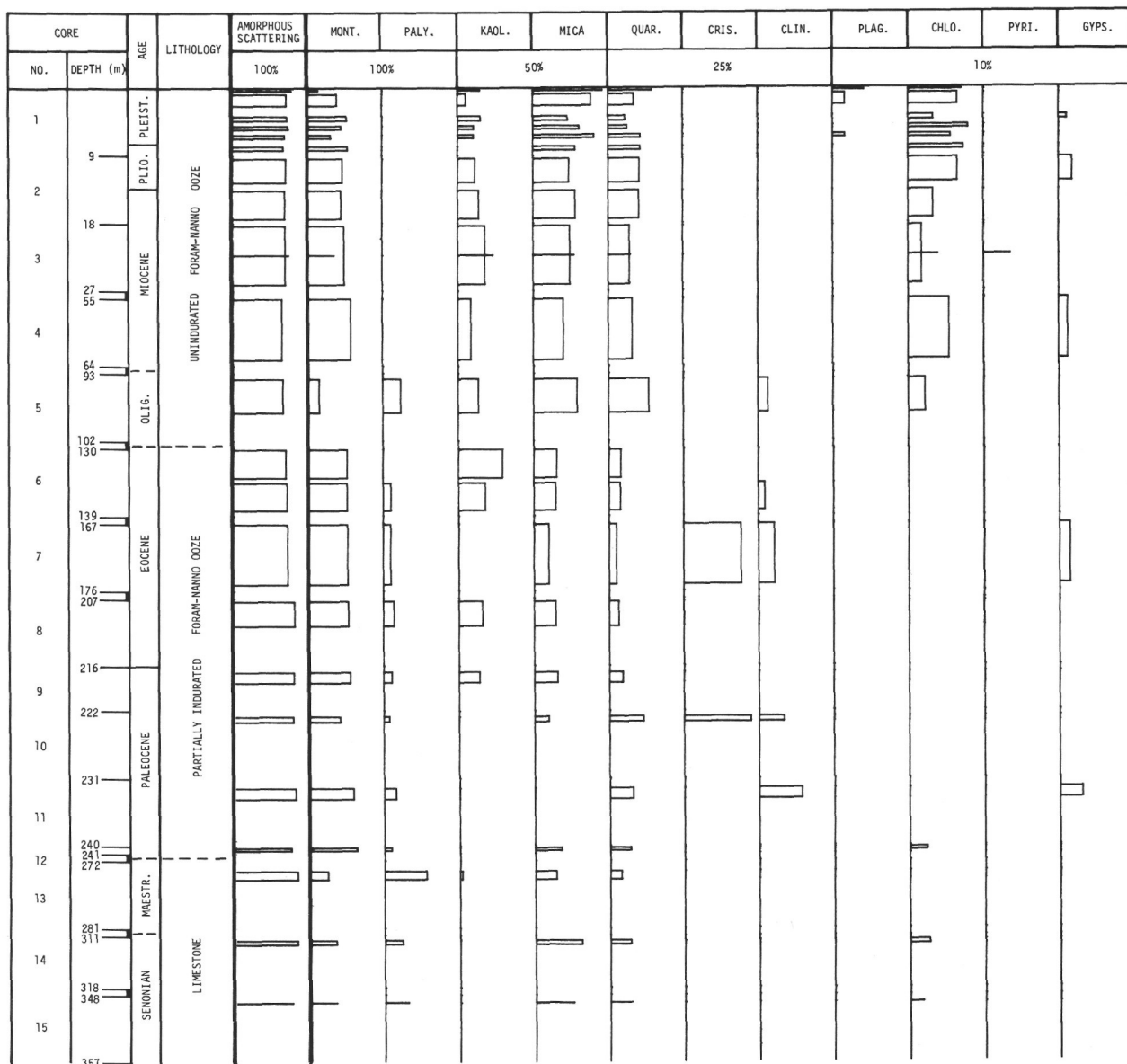


Figure 2. Hole 98, <math><2\mu\text{m}</math>.

Middle Unit (Cores 6-12)

The middle unit consists of a partially indurated foraminiferal-nannoplankton ooze and is Late Eocene to Middle Paleocene in age. This unit is mineralogically distinct from the upper unit in the bulk samples by the general absence of mica, kaolinite, aragonite and dolomite and by a lower quartz content (Figure 1). In the lower cores which contain some limestones, mica and clinoptilolite were detected.

The occurrence of chert was noted in Cores 7 and 10 by the shipboard geologists. Sediments associated with this chert have cristobalite in the <math><2</math>-micrometer and 2 to 20-micrometers fractions of Cores 6, 7 and 10 and in the bulk fraction of Core 10. In Core 10 the

cristobalite is associated with an increase in quartz content in both the bulk sample and the <math><2</math>-micrometer fraction (Figures 1 and 2). Cores adjacent to 7 and 10 also contain clinoptilolite. Kaolinite occurs less frequently in this unit than in the upper unit but palygorskite is more abundant (Figure 2). No chlorite was detected.

Lower Unit (Cores 13-15)

This unit is a well-indurated limestone which is Late Cretaceous (Turonian to Maestrichtian) in age. Only calcite was detected in the bulk samples (Figure 1). Montmorillonite and mica are the dominant minerals of the clay fraction. Palygorskite and some chlorite are also present (Figure 2).

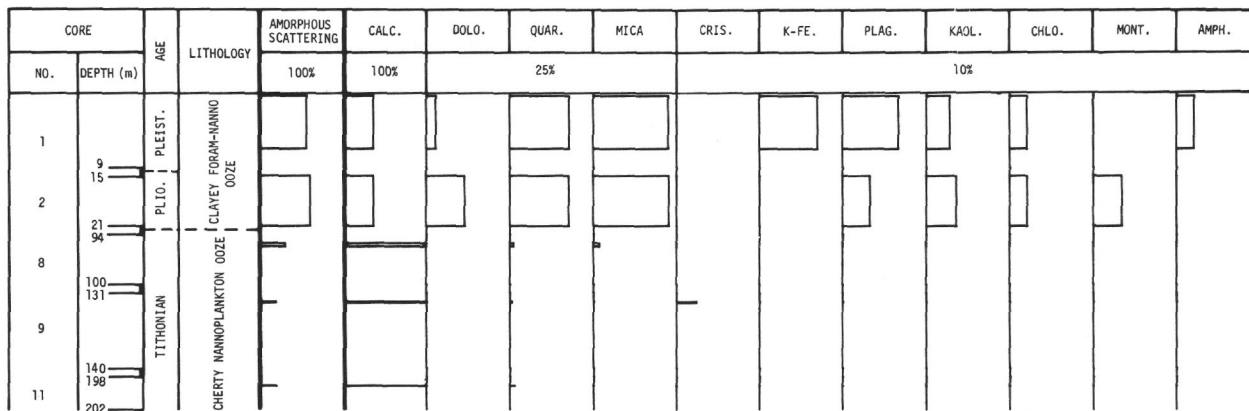


Figure 3. Hole 99A, Bulk.

The sediments of Site 98 are somewhat unusual inasmuch as only small quantities of quartz and very little feldspars were detected. Barite was detected in the silt fraction of Cores 7 and 9 (Table 1).

Site 99

Site 99 was located east of the Bahama Banks with the objective of recovering some of the oldest sediments in the Atlantic Ocean. Three sedimentary units and oceanic basalt were encountered.

Cores 1 and 2

These cores are a clayey foraminiferal-nannoplankton ooze, Pliocene-Pleistocene in age. Calcite, mica, and quartz are the dominant minerals in the bulk fraction. Plagioclase and small amounts of kaolinite and chlorite are present. Dolomite is present in the bulk sample but none was detected in the silt fraction. This implies that most of the dolomite particles are greater than 20 micrometers, or if smaller particles are present they are attached to, or are incorporated in, the greater than 20-micrometer particles.

The 2 to 20-micrometer fraction is predominantly composed of mica and quartz. A trace of clinoptilolite is seen in the Pleistocene sample. Mica and montmorillonite predominate in the <2-micrometer fraction (Figure 4; Table 2). Some palygorskite, kaolinite and chlorite are also present.

Cores 3-10

A cherty, partially indurated, nannoplankton ooze of Tithonian to Hauterivian age was recovered in this interval. Only three samples were submitted for X-ray analysis. These consist of calcite in the bulk sample with only minor quantities of quartz and cristobalite. Mica and quartz are the major components of the 2 to 20-micrometer fraction, and mica and montmorillonite dominate in the <2-micrometer fraction (Figure 4; Table 2). Cristobalite and clinoptilolite coexist in the 2

to 20-micrometer fraction as in Cores 7 and 10 in Hole 98. Some pyrite is indicated. By contrast with the overlying ooze, kaolinite, chlorite and palygorskite are notably absent in the <2-micrometer fraction. No samples of the lowermost red and green clayey Jurassic limestone or the underlying basalt were submitted for X-ray analysis.

Site 100

The location and objectives of Site 100 were similar to those of Site 99. The first core was taken at 203 meters. Continuous coring was begun below 237 meters.

Core 1

This core contains a plastic, nannoplankton ooze of Tithonian-Valanginian age. Quarts and Mica are the only nonbiogenous minerals detected in the bulk samples from this unit, and they are the major minerals in the 2 to 20-micrometer fraction (Figure 5; Table 3). The <2-micrometer fraction has an unusually high quartz content in contrast with Cretaceous sediments from Holes 98 and 99A and older sediments in Hole 100, but resembles the other samples in its montmorillonite and mica contents (Figures 2, 4 and 6). Chlorite and palygorskite are present but no kaolinite was detected.

Cores 2-5

A hard, clayey, Oxfordian limestone with red and green clay laminations was cored in this interval. In addition to large quantities of quartz and mica, the limestones contain some palygorskite, plagioclase and chlorite (Figure 5). Palygorskite appears in all samples in the <2-micrometer fraction and was frequently detected in the 2 to 20-micrometer fraction (Table 3). An occurrence of hematite is noted in Core 4. The silica phase of a chert sample from Core 3 consists mainly of quartz (Figure 6).

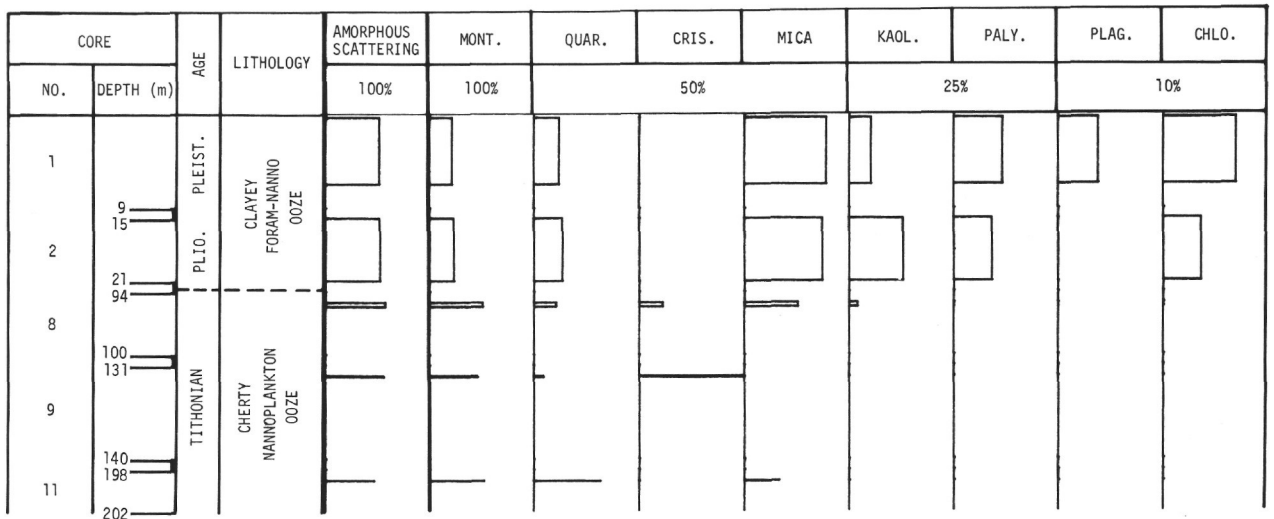


Figure 4. Hole 99A, <math><2\mu\text{m}</math>.

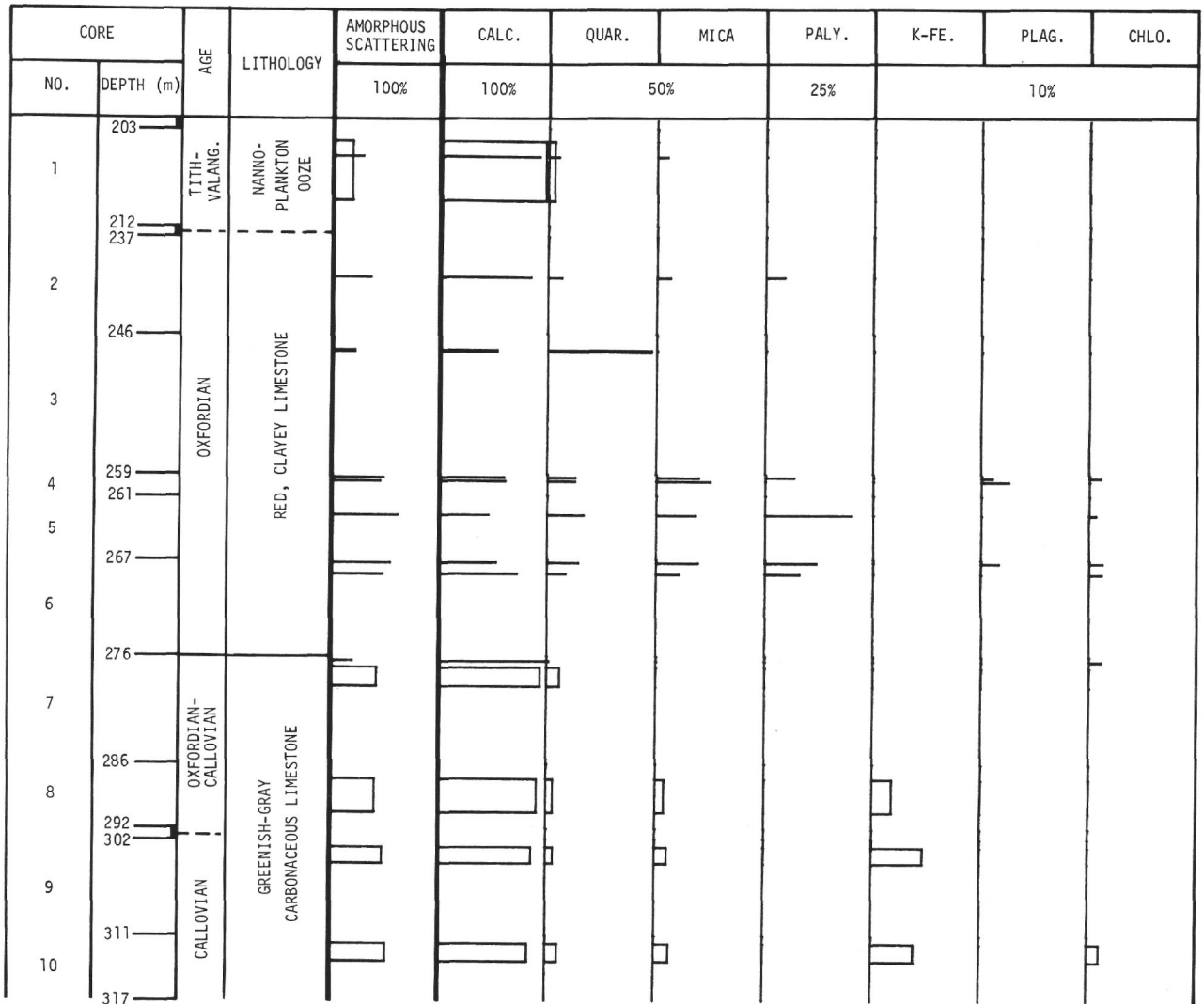


Figure 5. Hole 100, Bulk.

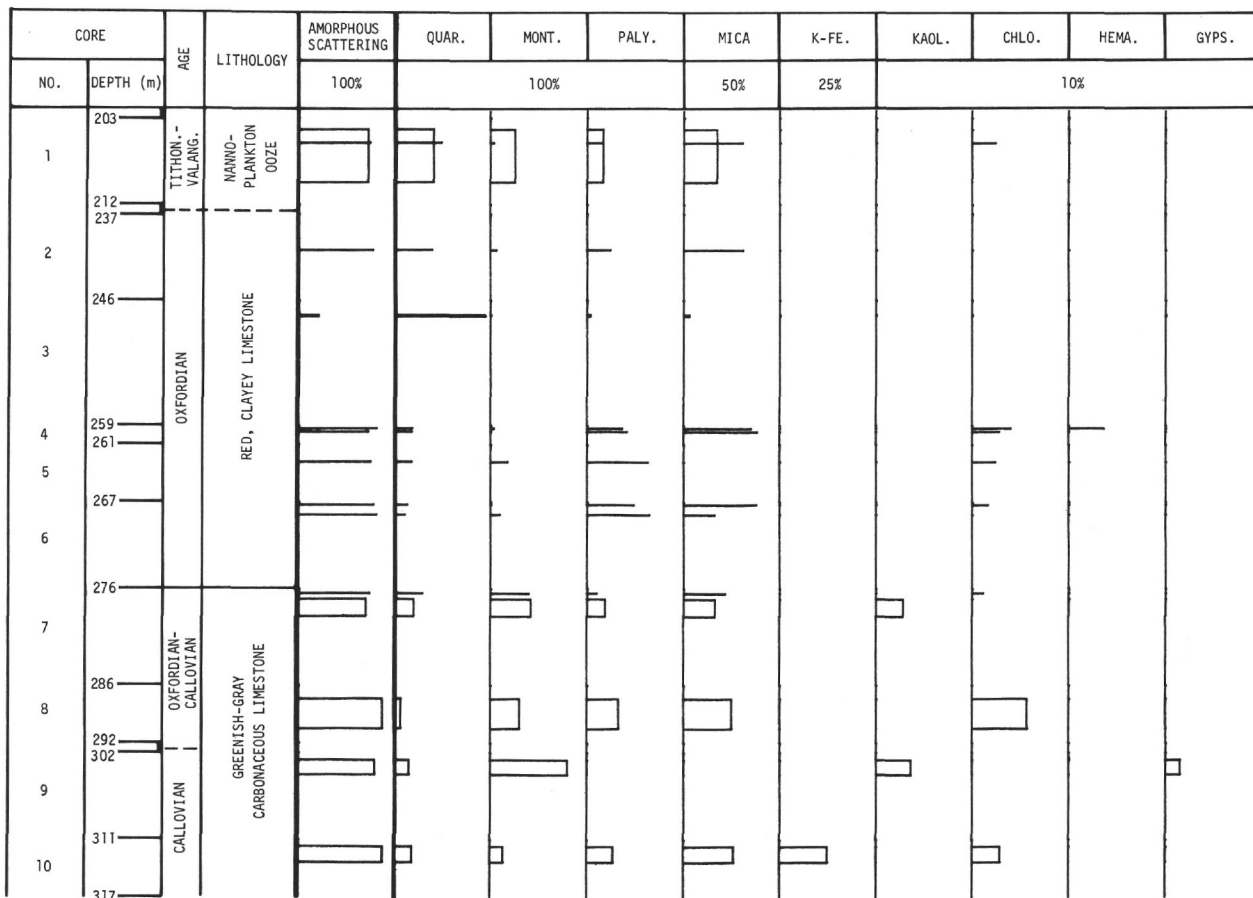


Figure 6. Hole 100, <2 μ m.

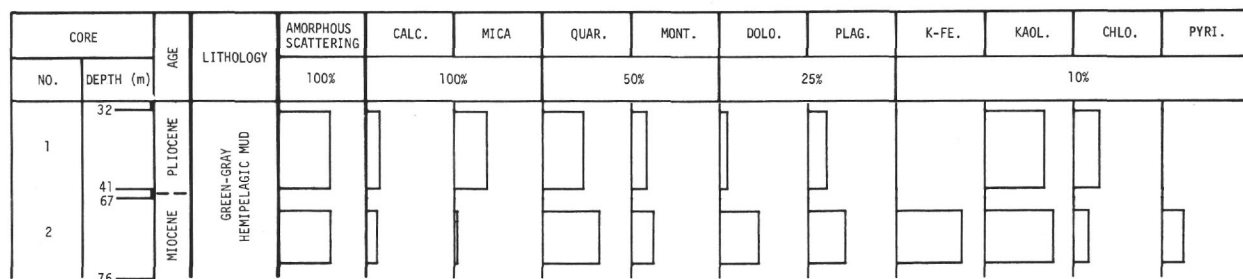


Figure 7. Hole 101, Bulk.

Cores 7-10

A greenish-gray micritic limestone of Middle to Late Jurassic age was found in these cores. The limestone is characterized by abundant carbonized plant debris, some of which has been replaced by pyrite. This limestone unit contains detectable quantities of mica and quartz in the bulk sample (Figure 5) which are also the major constituents of the 2 to 20-micrometer fraction (Table 3). K-feldspar occurs in Cores 8, 9, and 10 in the bulk, 2 to 20- and <2-micrometer fractions and appears to be restricted to this unit (Table 3). Some barite, pyrite and palygorskite are evident in the

2 to 20-micrometer fraction (Table 3). Mineralogically, the <2-micrometer fraction is very similar to the overlying red clayey limestones in Cores 2 through 6, except that kaolinite is present in the lower unit. Kaolinite is usually absent from Mesozoic sediments of Leg 11, and its presence in this lower unit is an unusual occurrence.

Site 101

Site 101 was located on a southerly spur of the Blake-Bahama Outer Ridge as a part of a study, along with Sites 102, 103, and 104, to better understand the

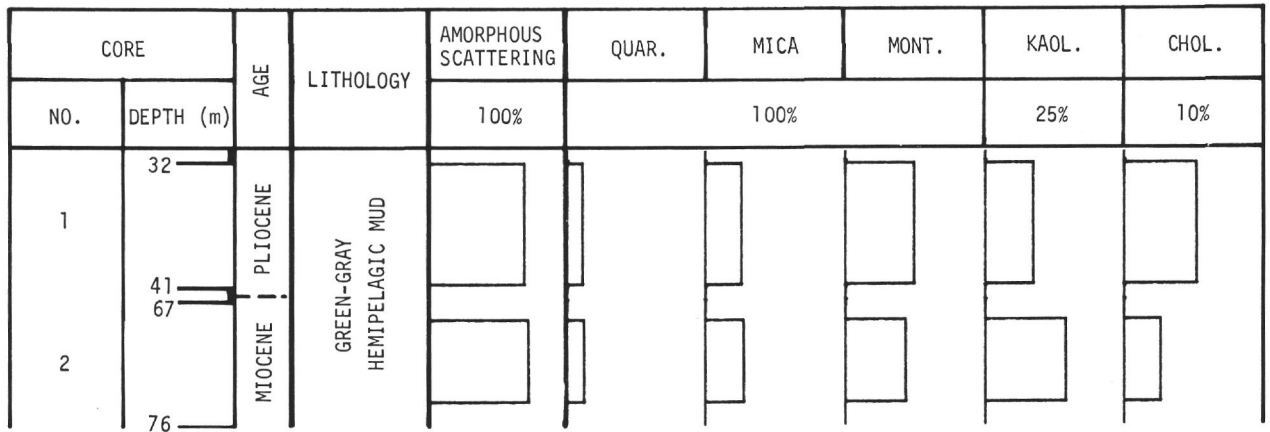


Figure 8. Hole 101, <math><2\mu\text{m}</math>.

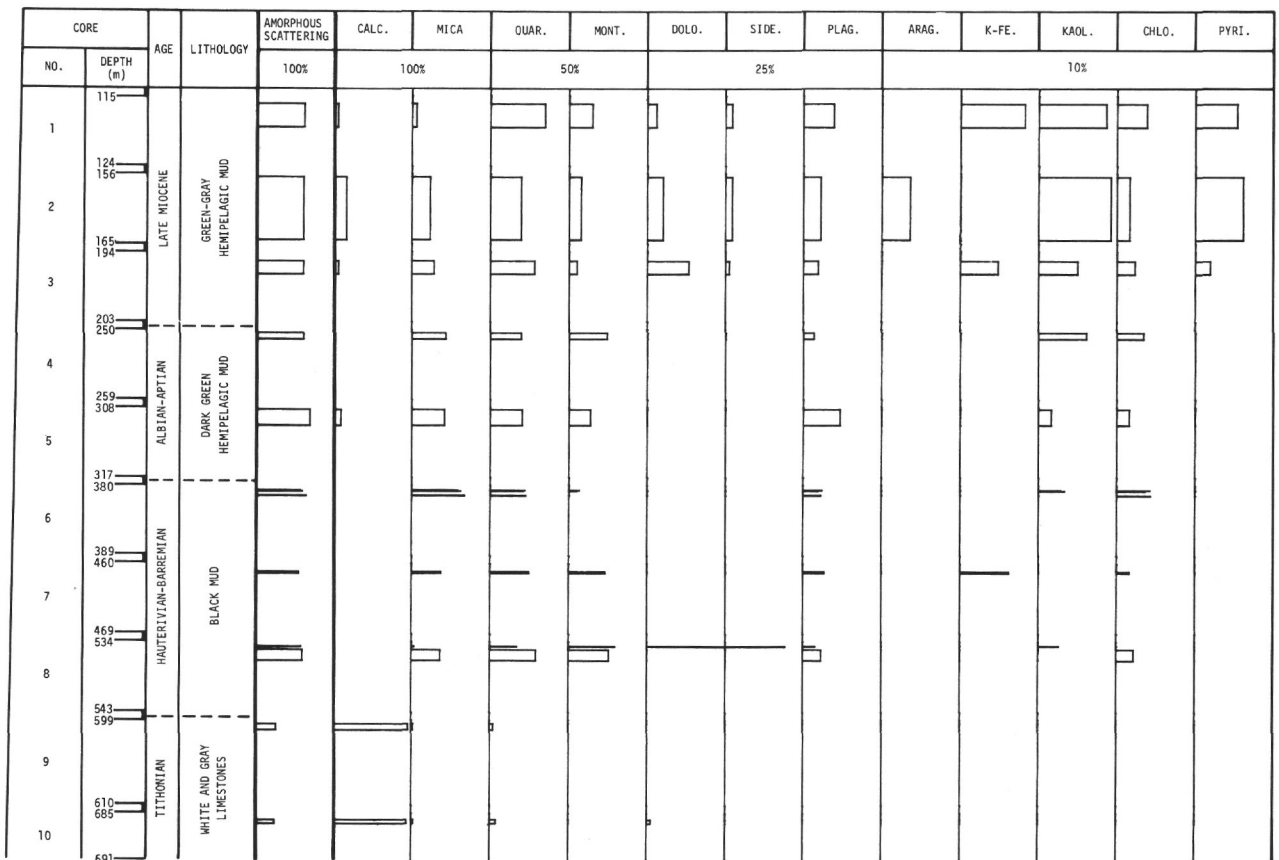


Figure 9. Hole 101A, Bulk.

origin of this physiographic feature. Four units were recognized by shipboard scientists in Holes 101 and 101A.

Greenish-Gray Mud

A Pliocene to Late Miocene, greenish-gray hemipelagic mud was recovered in Cores 1, 2, 1A, 2A and 3A. The mud closely resembles the sediments described by Ericson *et al.* (1961) from the continental margin of

North America with regard to the mineralogy, texture, sedimentary structures and color.

The bulk fraction contains a large number of minerals. Quartz and mica are the most abundant minerals in the bulk analyses and in the 2 to 20-micrometer fraction (Table 4), suggesting that the sediment is largely of a continental detrital origin. Dolomite, siderite, pyrite and aragonite are also present in this unit.

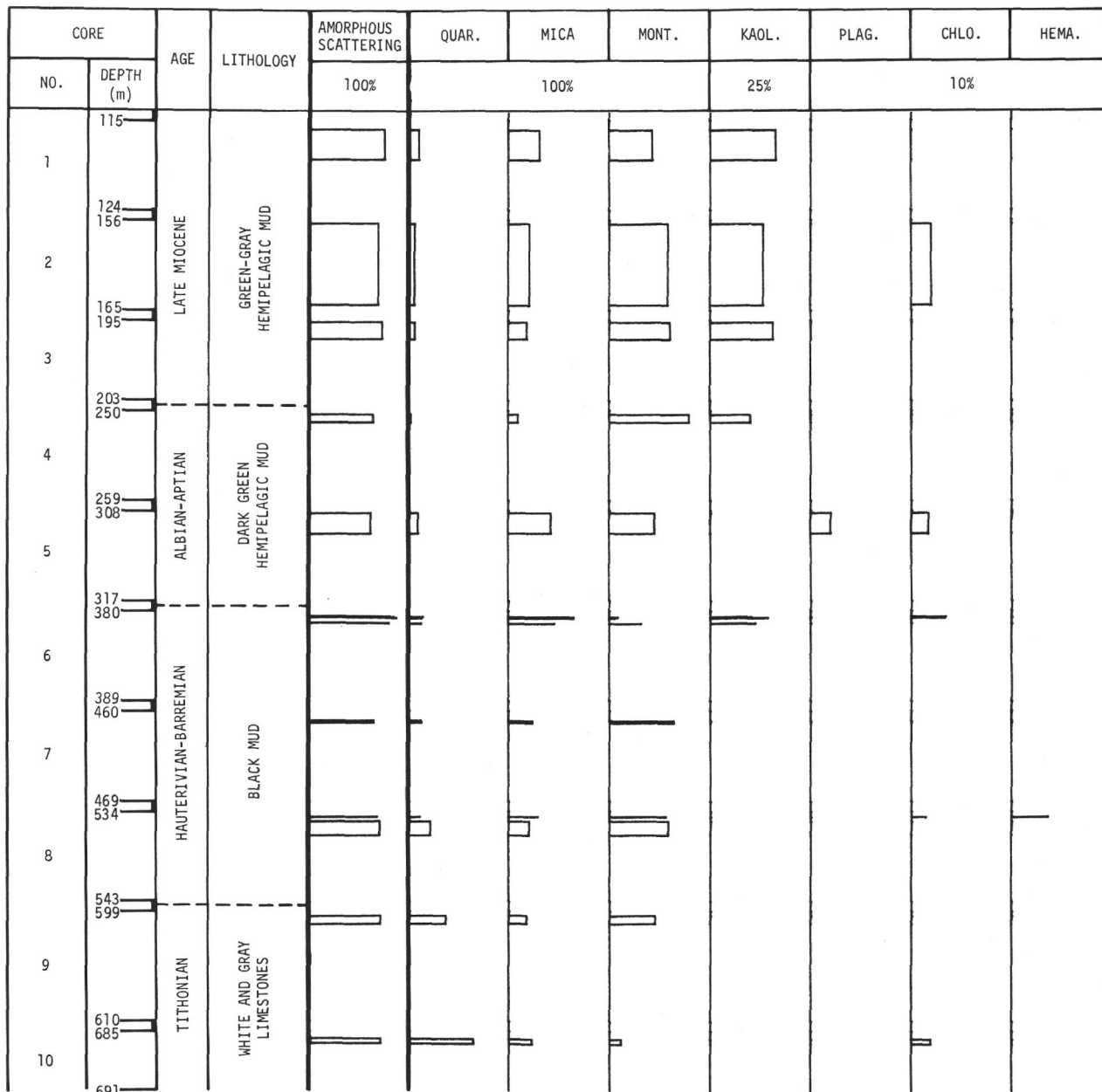


Figure 10. Hole 101A, <math><2\mu\text{m}</math>.

Clinoptilolite was found in the 2 to 20-micrometer fraction of Pliocene and Pleistocene sediments of Cores 1 and 2, in a similar mineral association as Core 1 in Hole 99. Montmorillonite is typically more highly concentrated in the <math><2</math>-micrometer fraction than mica in this unit (Figure 10; Table 4). Kaolinite persists throughout the unit.

Dark Green Mud

A dark green Albian-Aptian hemipelagic mud was encountered in Cores 4A and 5A. The detrital mineral assemblage in the bulk samples of this unit and the

overlying unit are similar, but this lower unit contains no dolomite, siderite, pyrite or K-feldspar and is less calcareous. The two hemipelagic mud units have similar mineral assemblages in the <math><2</math>-micrometer fraction.

Black and Dark Green Clay

A black and dark-green, carbonaceous clay of Barremanian to Valanginian age was found in Cores 6A to 8A. Carbonaceous matter, pyrite, siderite and the absence of calcite characterize this unit. In the bulk and 2 to 20-micrometer fractions this unit resembles the overlying green mud units except that there are occurrences of siderite and dolomite in Core 8A and an occurrence

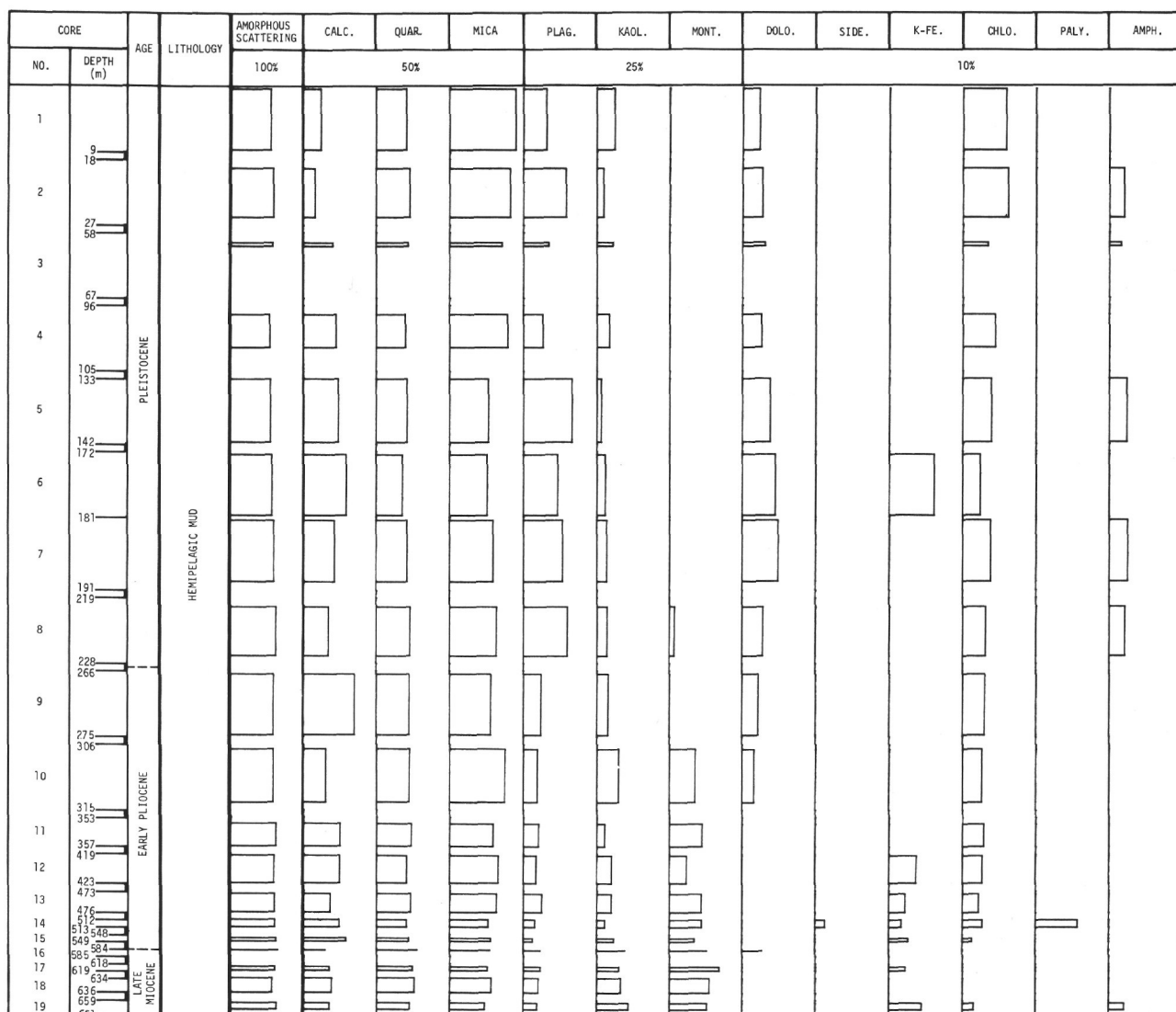


Figure 11. Hole 102, Bulk.

of K-feldspar in Core 7A (Figure 9; Table 4). As in the above units, mica and montmorillonite predominate in the <2-micrometer fraction (Figure 10). Kaolinite and chlorite occur in lesser amounts. Traces of pyrite were found in the 2 to 20-micrometer fraction (Table 4).

White Limestone

A sequence of white and gray, thinly-bedded limestones of Tithonian age was recovered in Cores 9A and 10A. Only traces of quartz, mica and dolomite were detected in the bulk samples (Figure 9). Quartz and mica make up the major proportion of the decalcified 2 to 20-micrometer fraction as is typical of the Atlantic sediments. Pyrite is present. Quartz, mica and montmorillonite are the major minerals in the <2-micrometer fraction; kaolinite was not detected (Figure 10).

Sites 102, 103 and 104

Holes 102, 103 and 104 were drilled across the Blake-Bahama Outer Ridge with the objective of providing data concerning the origin of the ridge. The sediment recovered at these sites is a greenish hemipelagic mud resembling the green muds described by Ericson *et al.* (1961). Specific lithologic units could not be established by the shipboard scientists, and the sediments were subdivided according to age.

Pleistocene

Pleistocene sediments were found at all three sites. The best developed section was in Hole 102 (Cores 1 to 8) at the crest of the ridge. In Holes 103 and 104, on opposite flanks of the ridge, only a few meters of Pleistocene sediments were found and were sampled for X-ray mineralogy in the top two samples of each hole (Figures 11 to 16; Tables 5 to 7).

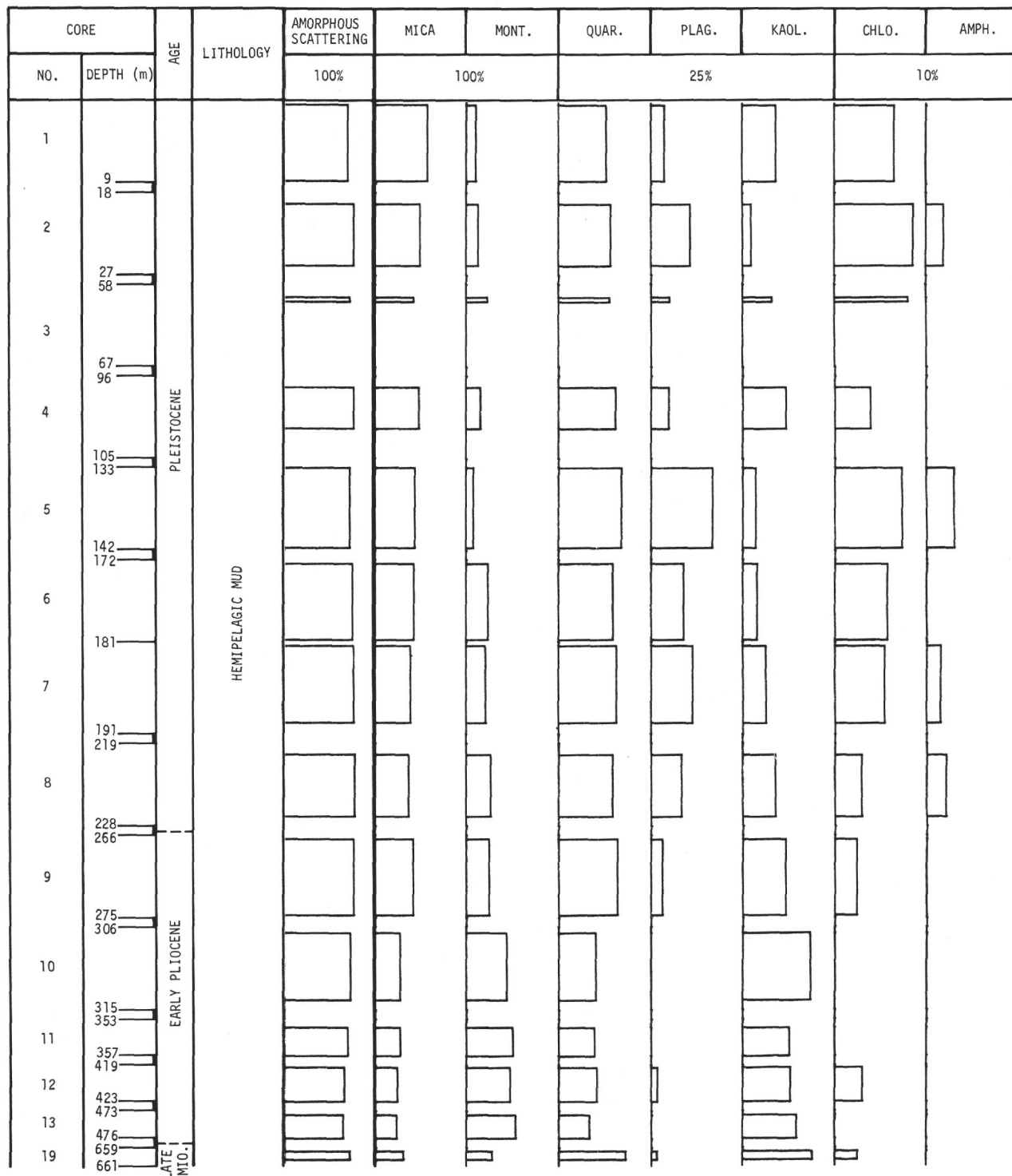


Figure 12. Hole 102, <math><2\mu\text{m}</math>.

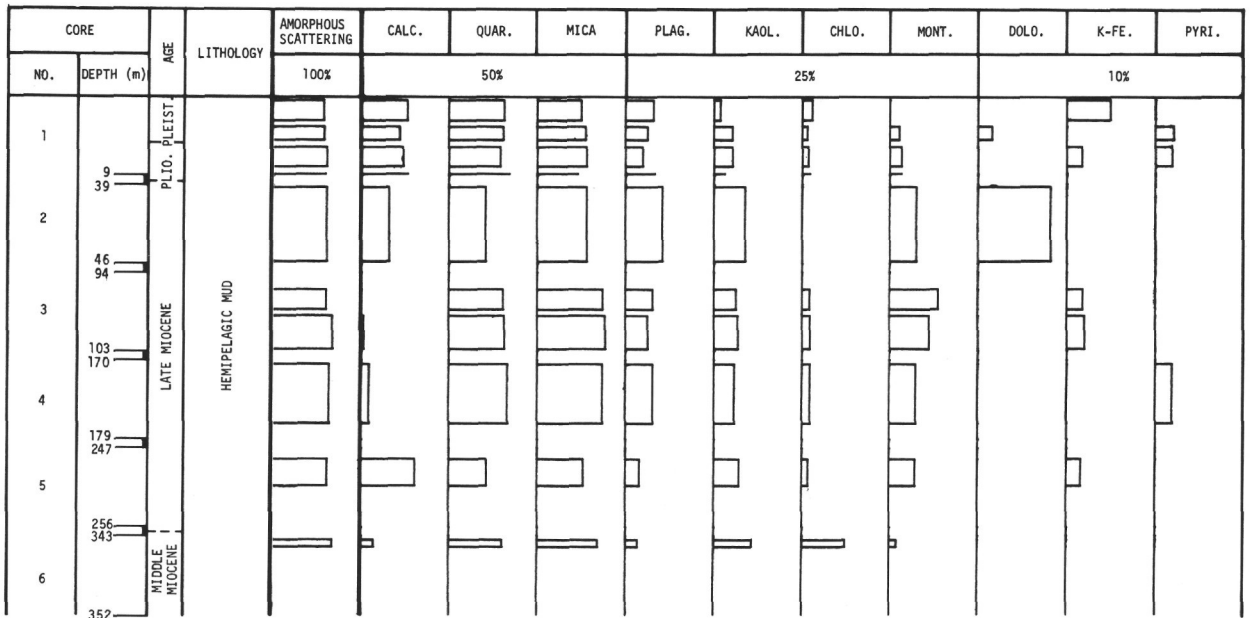


Figure 13. Hole 103, Bulk.

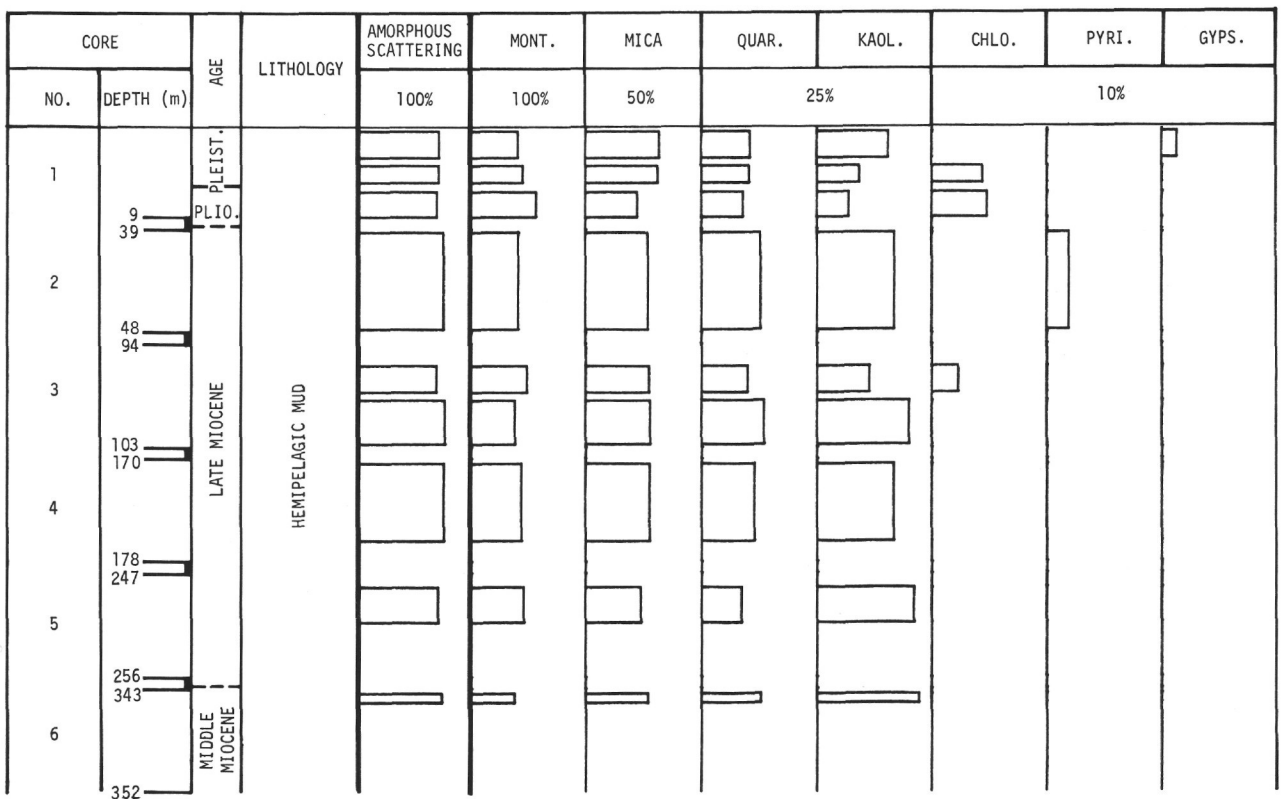


Figure 14. Hole 103, <math><2\mu\text{m}</math>.

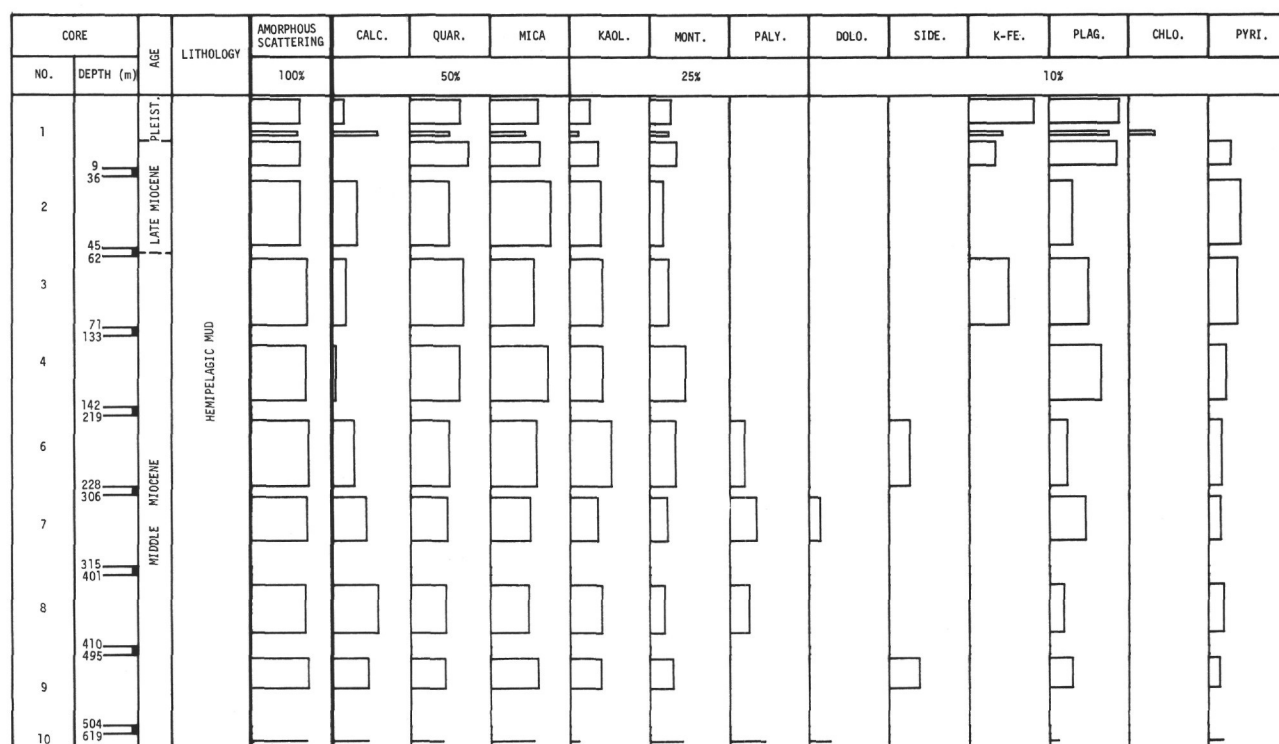


Figure 15. Hole 104, Bulk.

Mica, calcite and quartz form the dominant minerals of the sediments (Figures 11, 13 and 15). Plagioclase, kaolinite, chlorite and dolomite persist throughout the unit. Amphibole was detected in several cores. Montmorillonite does not occur in detectable amounts in the bulk sample of Hole 102, and it occurs in low concentrations in the <2-micrometer fraction.

The 2 to 20-micrometer fraction consists mainly of mica and quartz. Traces of pyrite occur throughout the unit. The composition of the <2-micrometer fractions reflects the composition of the bulk samples except that dolomite was not detected.

Pliocene-Late Miocene

Sediments of the Pliocene-Late Miocene unit were recovered in Cores 8 to 19 in Hole 102, Cores 1 to 5 in Hole 103 and in Cores 1 and 2 in Hole 104. Mineralogically no conspicuous change is evident at the Plio-Pleistocene boundary but there is a gradual change in mineralogy over Cores 8, 9 and 10 in Hole 102 (Figures 11 and 12).

The dolomite content diminishes with depth in Hole 102 and is rarely found in the Pliocene-Late Miocene unit (Figure 11). Montmorillonite was first detected in Pliocene-Pleistocene sediments and continues downward into the Late Miocene sediments (Figure 11). It also becomes a more prominent constituent in the <2-micrometer fraction below the Pliocene-Pleistocene boundary.

The content of chlorite, mica and plagioclase appears to diminish with depth in Hole 102 (Figures 11 and 12). In the <2-micrometer fraction, the frequency of detection of chlorite and plagioclase becomes less with depth (Figure 12). No amphibole was detected below the Pliocene-Pleistocene boundary in the <2-micrometer fraction (Figure 12).

Throughout this unit, mica and quartz are the predominant minerals of the 2 to 20-micrometer fraction. The frequency of pyrite occurrence may be higher in this unit than in the overlying Pleistocene unit. Clinoptilolite occurs in trace amounts restricted to the Pliocene-Late Miocene unit (Tables 5 and 6) in Cores 102 and 103.

Middle Miocene

Middle Miocene sediments were recovered only at the bottoms of Holes 103 and 104. The sediment is a green hemipelagic clay, as above, but limestone fragments occur in Hole 104. Mineralogically there is no distinction between the Pliocene-Late Miocene unit and the Middle Miocene unit except that small amounts of palygorskite, dolomite and siderite are detected in some bulk samples in the Middle Miocene unit. Pyrite is abundant throughout the unit in the bulk and 2 to 20-micrometer samples (Figures 13 and 15; Tables 6 and 7).

Several possible mineral trends, which might be correlated, occur in Sites 102, 103 and 104. For example, a

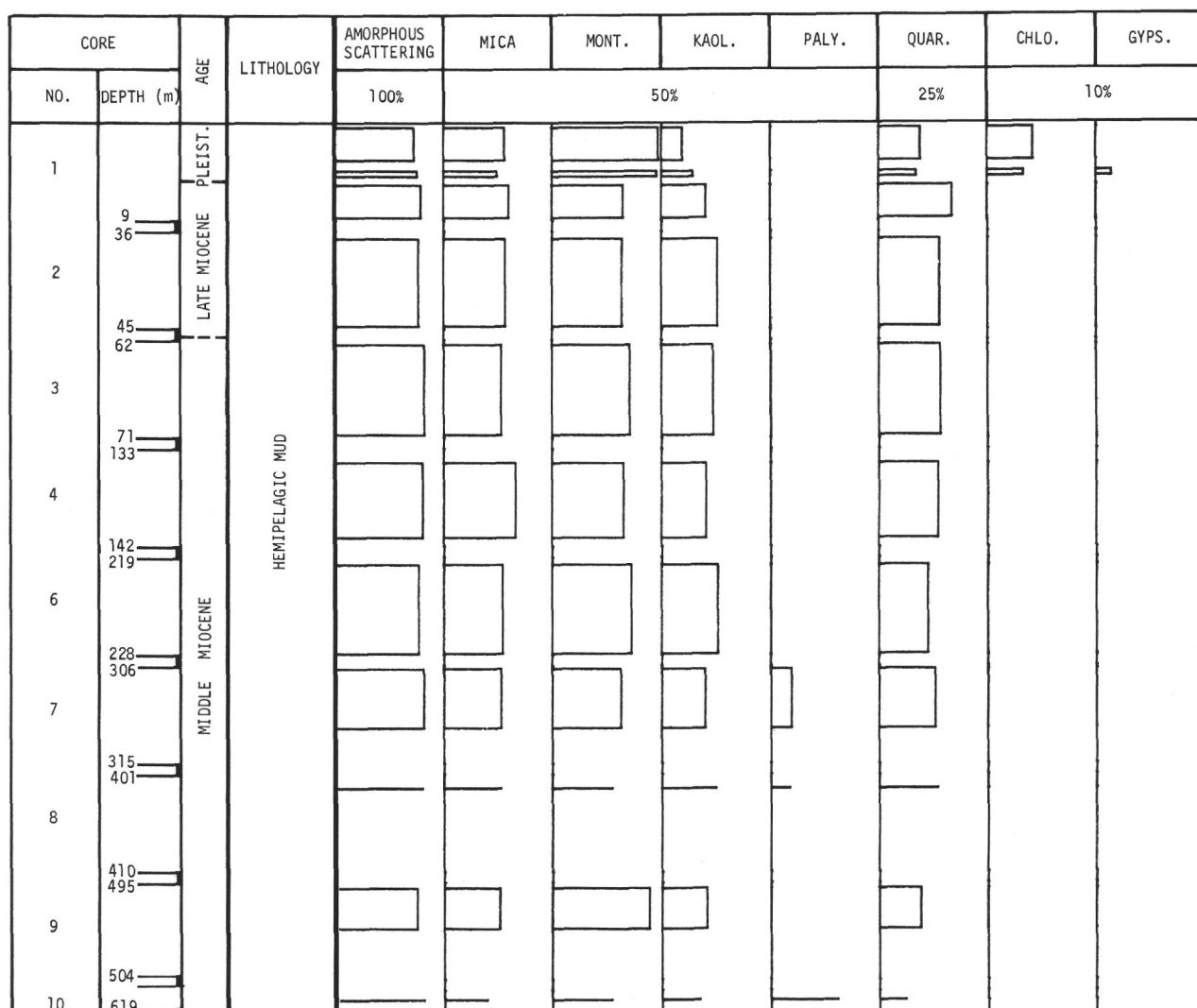


Figure 16. Hole 104, <2 μ m.

zone of clinoptilolite occurrence exists in Miocene sediments. The chlorite content diminishes with depth, especially at Site 102, and ultimately goes below detection in Middle Miocene sediments (Figures 11 to 16).

Site 105

Hole 105 was drilled in the continental rise hills at the bottom of the continental rise between Bermuda and New York. The objectives were to study the origin of the hills and to ascertain the lithologic composition of seismic reflecting layers (Horizons A and β). A nearly complete section was recovered which bottomed in basalt. These sediments were divided into six units by the shipboard geologists.

Cores 1-3

A Holocene-Pleistocene-Pliocene, greenish-gray hemipelagic mud, similar to widespread muds of the continental margin, was recovered in this unit. The

major minerals present in the bulk and 2 to 20-micrometer fractions are mica and quartz (Figure 17, Table 8). Kaolinite and montmorillonite are frequently found. As at Sites 102, 103 and 104, montmorillonite was not detected in the Pleistocene bulk samples and is considerably less abundant in the <2-micrometer fraction than in the older units. Both this unit and the underlying unit reportedly contain high concentrations of plant debris.

Cores 4-10

This unit consists of multicolored, thinly-bedded clays of unknown age. According to shipboard smear slide analyses, this unit contains large quantities of zeolites, pyrite, siderite, and possibly rhodochrosite and sphalerite. Large quantities of clinoptilolite were found in Core 5, such that it forms the major constituent of the 2 to 20-micrometer fraction (Figures 17 and 18; Table 8). Pyrite was detected only in a few samples. The other minerals were not detected.

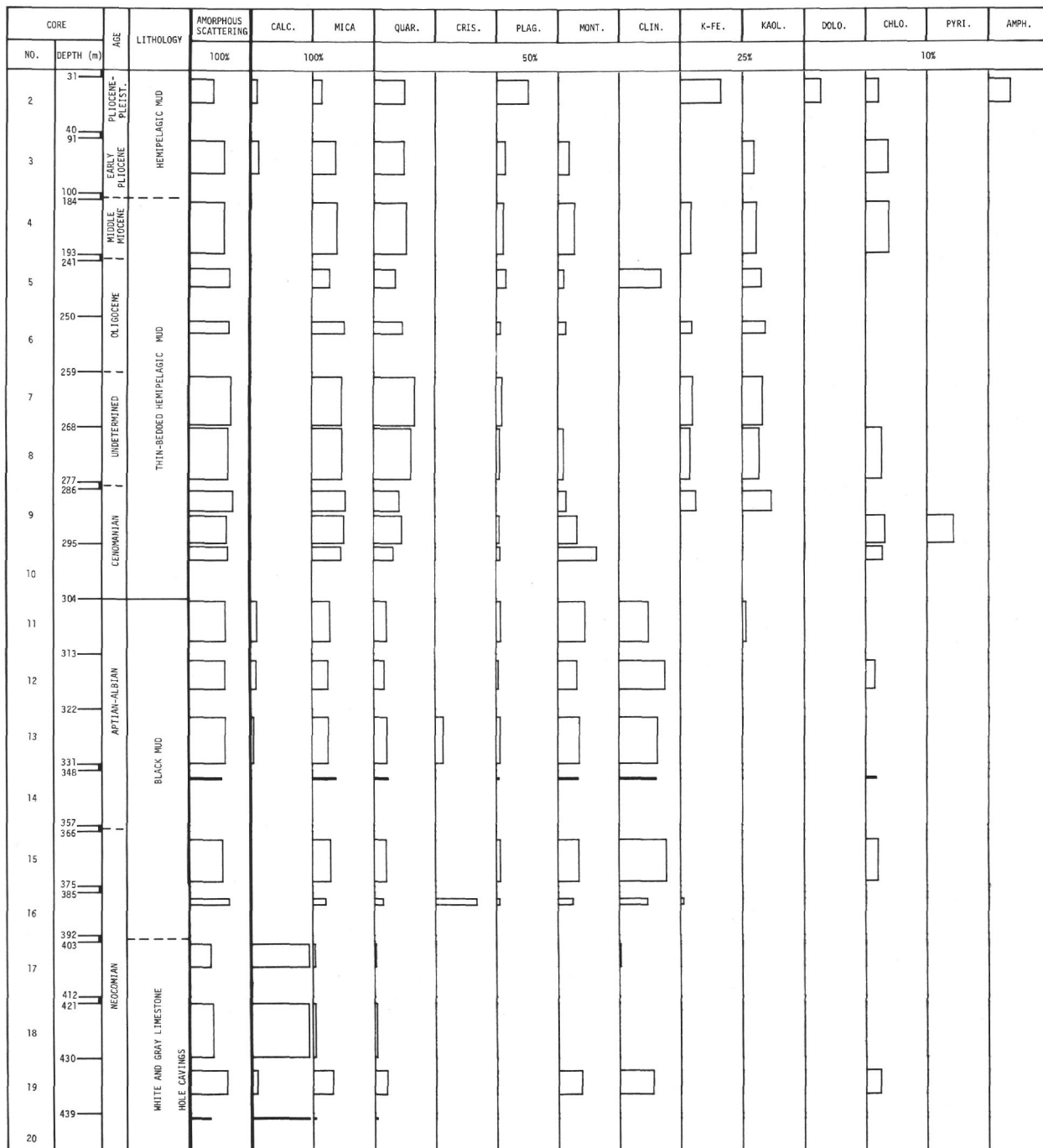


Figure 17. Hole 105, Bulk.

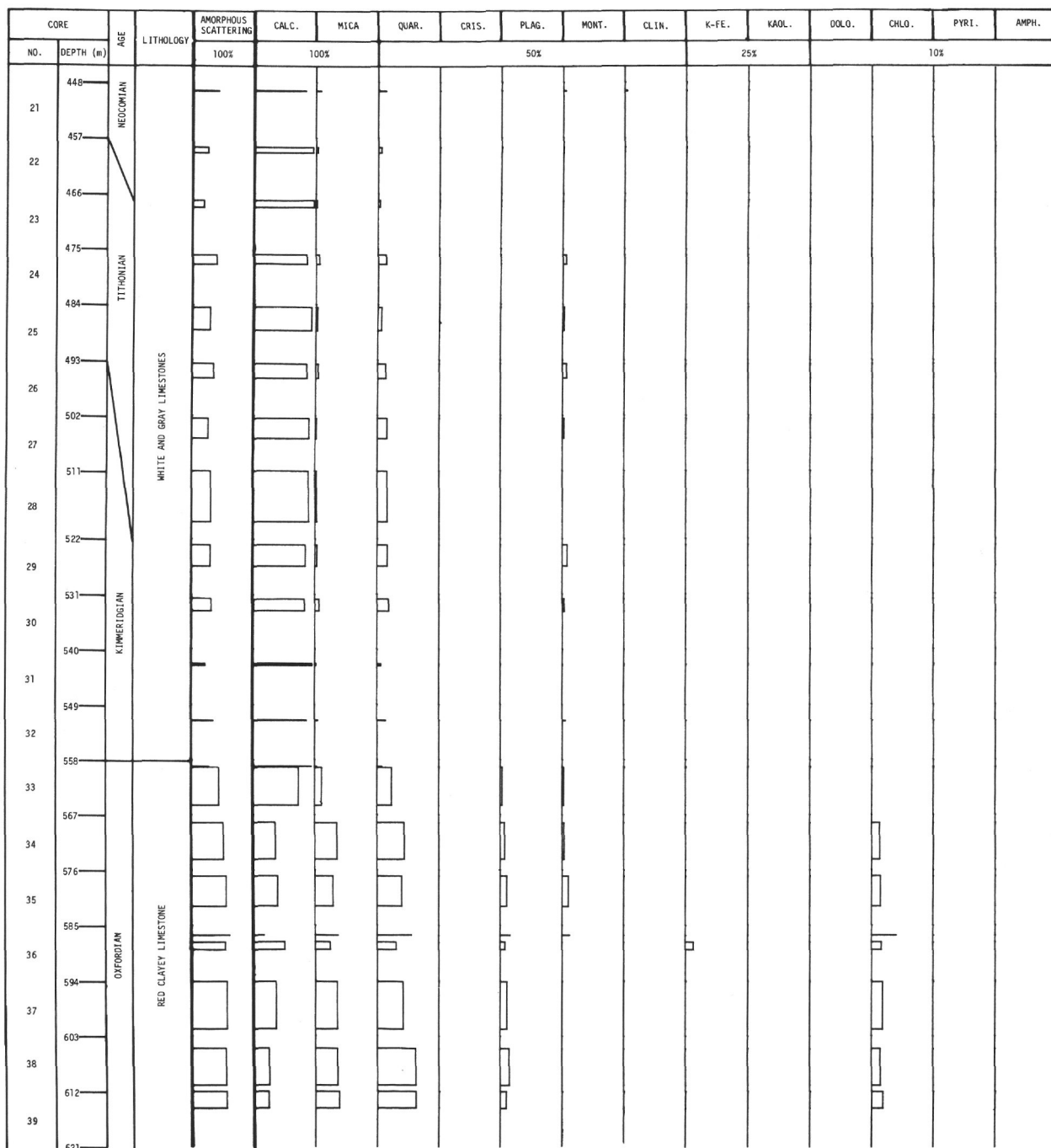


Figure 17. (Continued)

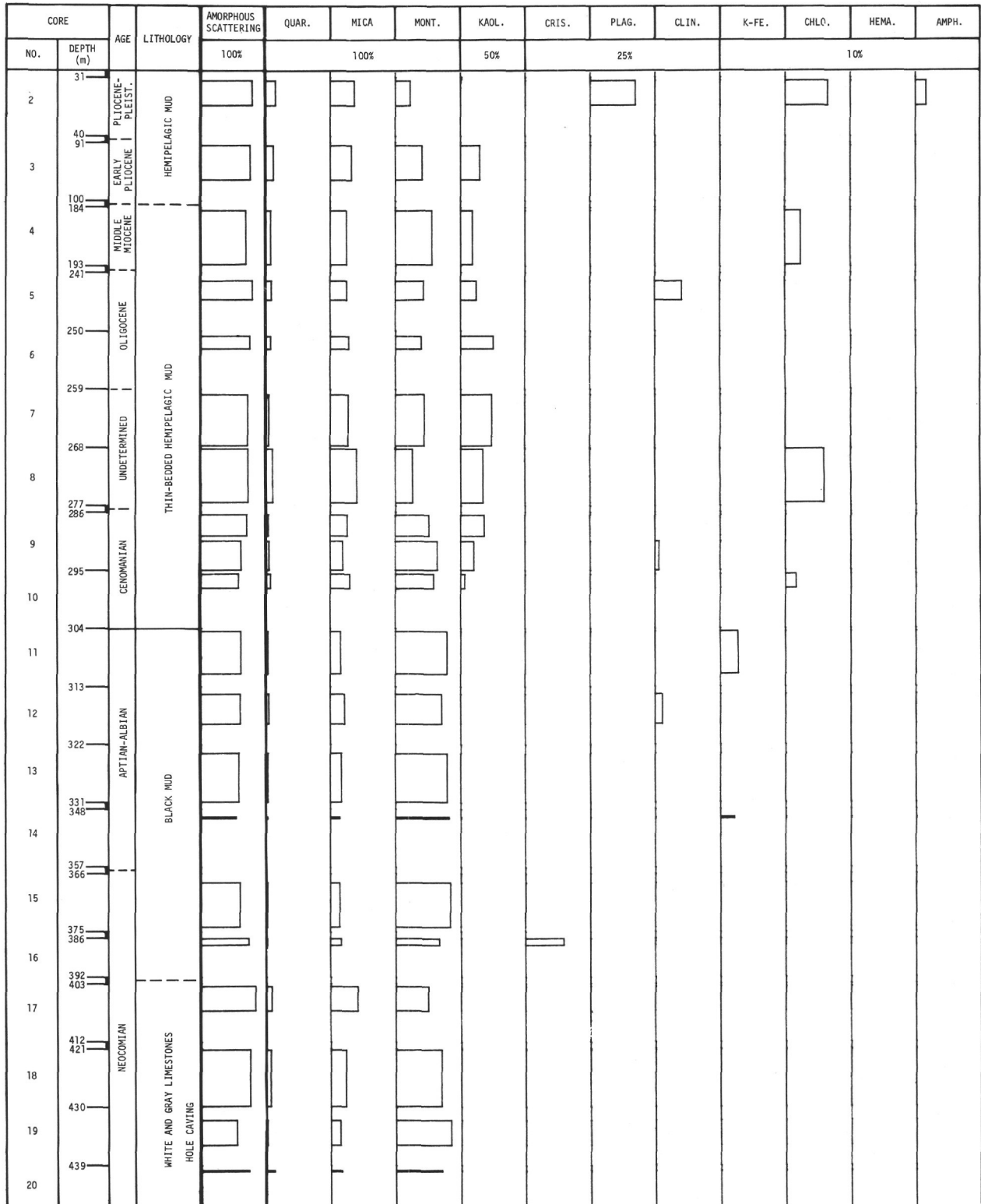


Figure 18. Hole 105, <math><2\mu\text{m}</math>.

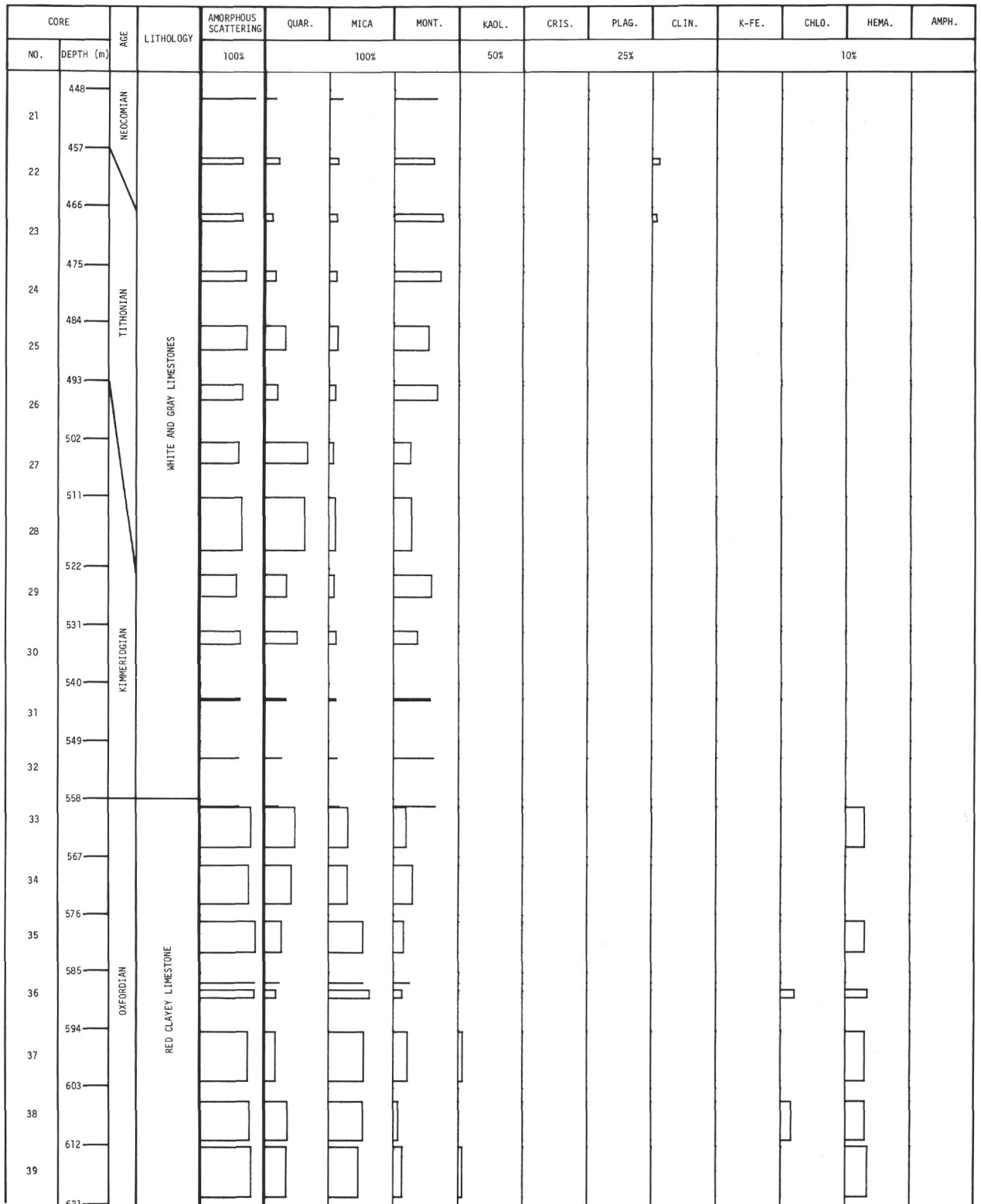


Figure 18. (Continued)

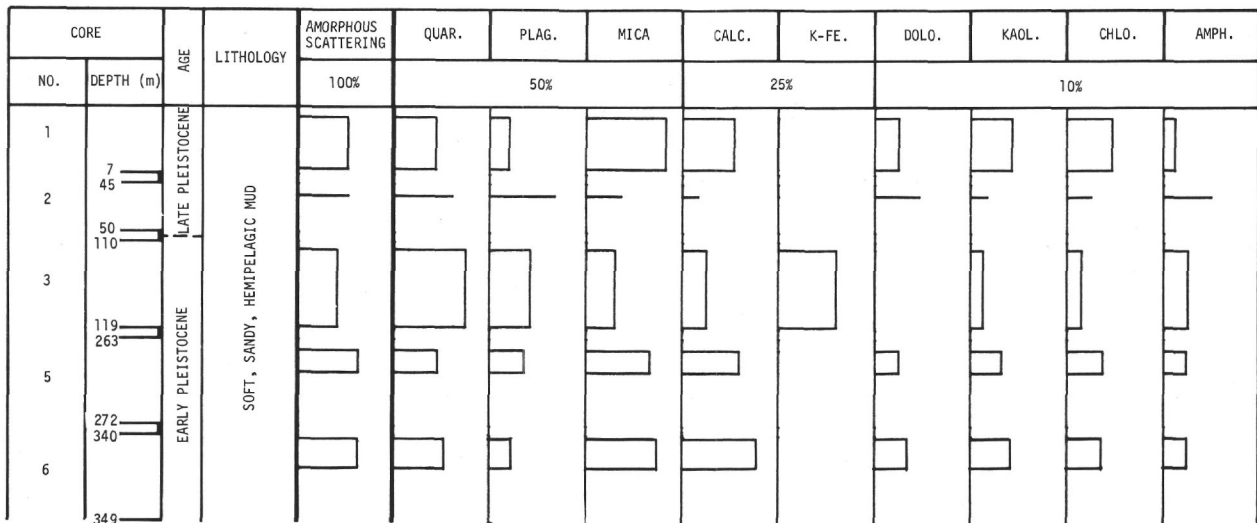


Figure 19. Hole 106, Bulk.

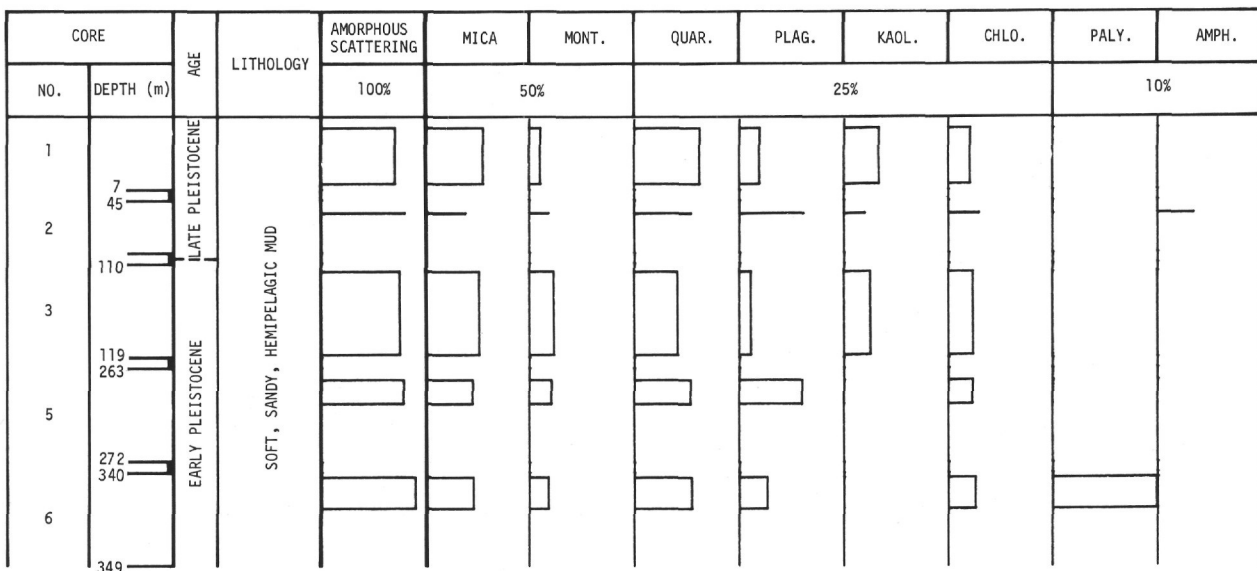


Figure 20. Hole 105, <2μm.

Cores 11-16

A massively-bedded black mud, high in carbonaceous material of Albian-Aptian age and similar to the carbonaceous unit at Site 101, was recovered in Cores 11 through 16. The detrital minerals quartz, mica and plagioclase persist throughout the black mud unit. No K-feldspar was detected. Clinoptilolite, pyrite and cristobalite were detected in this unit by the X-ray analysis. Clinoptilolite is abundant in the bulk samples (Figure 17) and forms the major constituent of the 2 to 20-micrometer fraction. The montmorillonite concentration in the black mud unit is higher than in the overlying units. Kaolinite and chlorite were detected infrequently in the bulk samples, but are absent from the <2-micrometer fraction (Figure 18).

Cores 17-32

The fourth lithologic unit consists of alternating white, massively-bedded and greenish-gray, laminated, clayey limestone beds. The age of this unit is Tithonian-Neocomian. The bulk fraction, besides calcium carbonate, contains only traces of mica, quartz and montmorillonite (Figure 17). The decalcified 2 to 20-micrometer fraction consists primarily of mica and quartz (Table 8). Clinoptilolite and pyrite were detected more frequently and are generally more abundant in the upper portion of the unit; they correlate with a higher frequency of occurrence of the greenish-gray, clayey limestone in the upper portion. Mica and montmorillonite are the only clay minerals found in the <2-micrometer fraction. The average

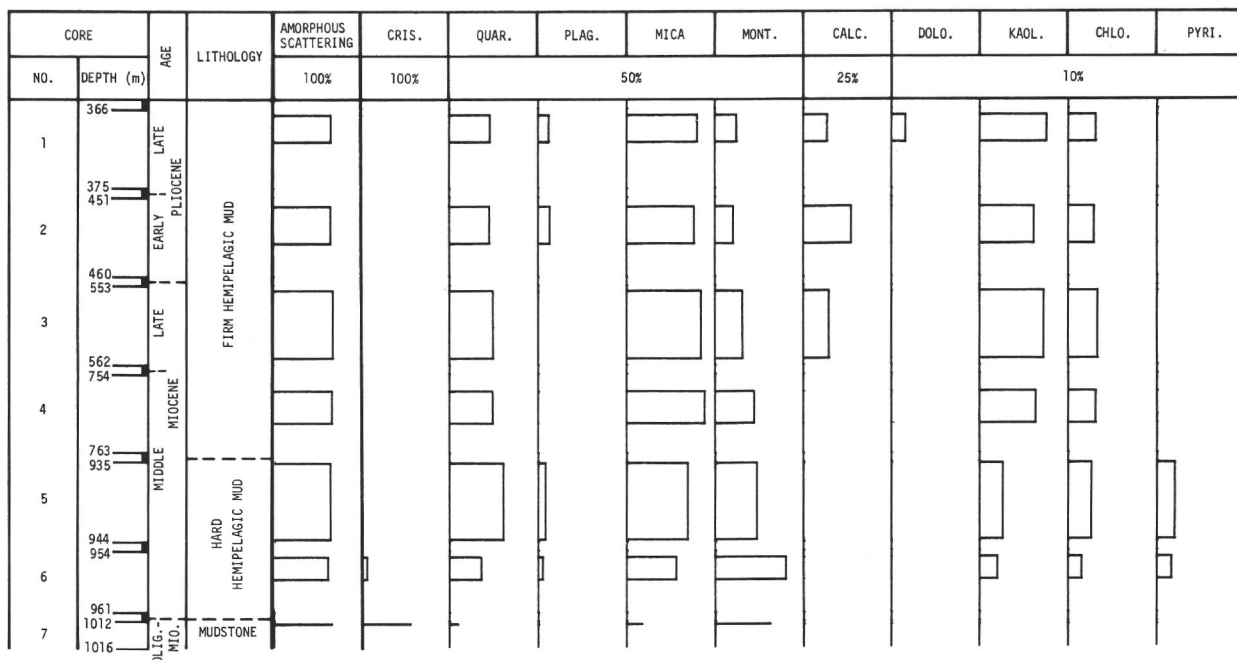


Figure 21. Hole 106B, Bulk.

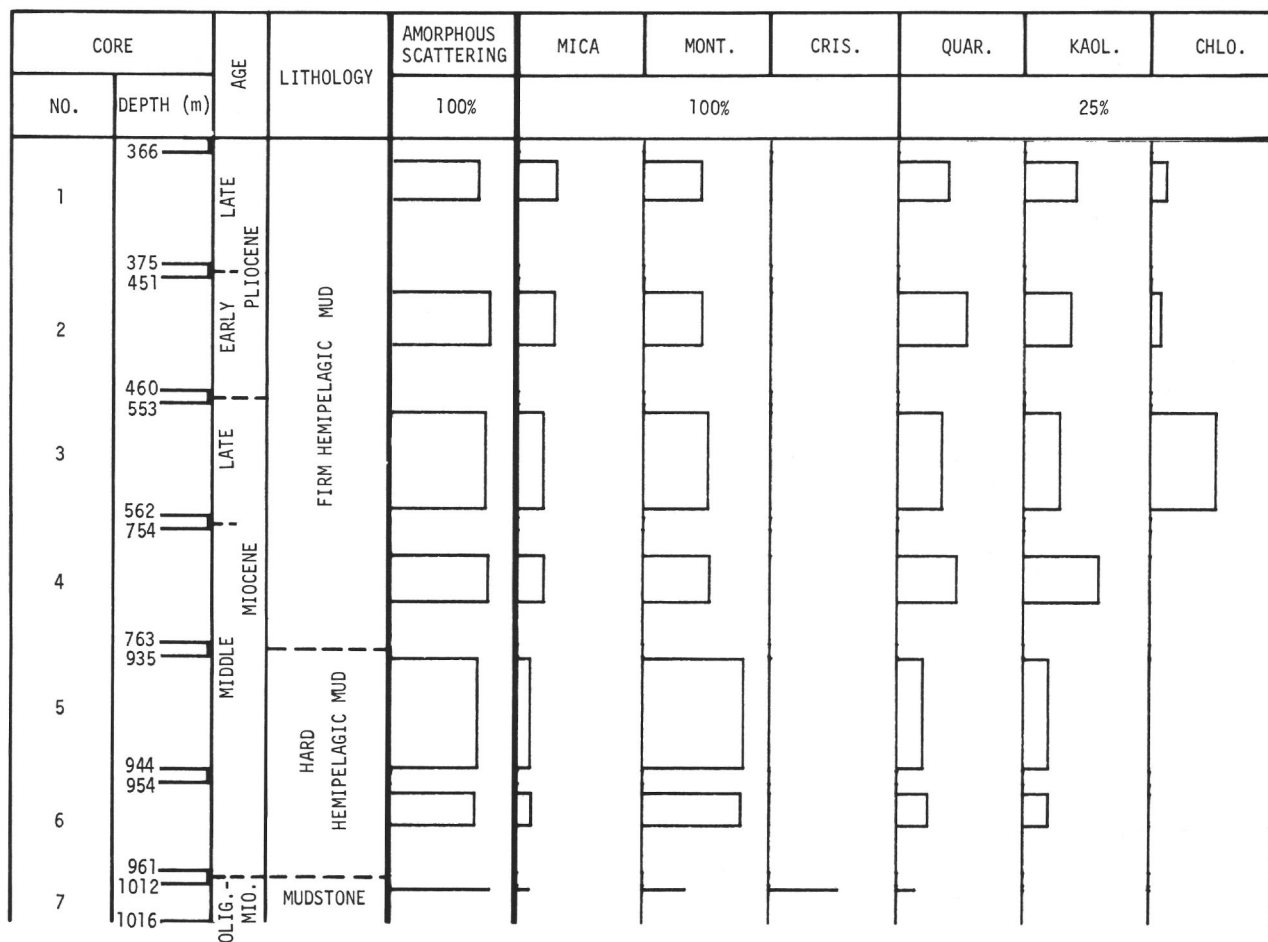


Figure 22. Hole 106B, <2µm.

CORE		AGE	LITHOLOGY	AMORPHOUS SCATTERING	CALC.	QUAR.	K-FE.	PLAG.	MICA	DOLO.	ARAG.	KAOL.	CHLO.	MONT.	AMPH.
NO.	DEPTH (m)			100%	100%	50%	25%			10%					
1	39	MIDDLE EOCENE	CALCAREOUS SILTICEOUS OOZE												
	57														
2	75	?	?												

Figure 23. Hole 108, Bulk.

CORE		AGE	LITHOLOGY	AMORPHOUS SCATTERING	MICA	MONT.	QUAR.	KAOL.	PLAG.	CHLO.	AMPH.
NO.	DEPTH (m)			100%	100%		25%		10%		
1	39	MIDDLE EOCENE	CALCAREOUS SILTICEOUS OOZE								
	57										
2	75	?	?								

Figure 24. Hole 108, <2 μ m.

montmorillonite content may exceed the mica content. The quartz content in the <2-micrometer fraction shows a marked fluctuation in this unit (Figure 18).

Cores 33-39

A red, clayey, Oxfordian limestone with green laminations was recovered in Cores 33 to 39. Calcite, mica and quartz occur in approximately equal proportions. Minor amounts of plagioclase, K-feldspar and chlorite are present. The 2 to 20-micrometer fraction consists mainly of mica and quartz and also contains a minor occurrence of clinoptilolite. The <2-micrometer fraction largely consists of quartz, mica and montmorillonite, as above, but with mica predominating over the montmorillonite (Figure 18, Table 8). Kaolinite and chlorite were detected at scattered locations. Hematite, which gives the limestone its characteristic color (Lancelot *et al.*, this volume) was detected in nearly every sample (Figure 18).

No unusual mineralogic assemblage was noted in Core 38, where native copper was found (see section on special samples below).

Samples from the sixth unit, which consists of pyroclastic sediments and basalt, were not submitted for X-ray mineralogic analysis.

Site 106

Site 106 was located in a body of continental rise sediments which is composed of hemipelagic mud. This mud was divided by the shipboard geologists into four lithologic units primarily on the basis of induration. Cores 1 to 6 contain a soft hemipelagic mud of Quaternary age. A firm, Pliocene to Middle Miocene mud was recovered in Cores 1B to 4B. Hard mud of Middle Miocene age was recovered in Cores 5B and 6B. Cores 7B and 8B contained a highly indurated, fissile mudstone of Oligocene to Miocene age.

Mineralogically, the sediments at Site 106 appear to be one continuous unit (Figures 19 to 22; Table 9). The detrital assemblage of quartz, mica and plagioclase persists uniformly throughout the unit. Calcite decreases continuously with depth. Amphibole appears to be restricted to the uppermost Quaternary unit.

The 2 to 20-micrometer fraction is primarily composed of mica and quartz throughout the recovered section. Pyrite may increase with depth in the section and is most abundant in the 2 to 20-micrometer fraction. Clinoptilolite is most prevalent in the second unit. Mica and montmorillonite are the predominant minerals in the <2-micrometer fraction (Figures 20 and 22). The mica content decreases continuously with depth while the montmorillonite content correspondingly increases. Kaolinite and chlorite were detected throughout the section in the bulk samples, but chlorite was detected only in the upper two units in the <2-micrometer fraction. Cristobalite and montmorillonite are major constituents in the basal mudstone unit.

Site 108

Site 108 was located on an Eocene outcrop on the continental slope. Little sediment was recovered. The sediment is a siliceous nannoplankton-foraminiferal ooze which contrasts sharply with correlative sediments farther down the continental slope.

A composited sample of the ooze shows a high calcite content (Figure 23). Small amounts of mica and quartz were detected. A trace of aragonite in the bulk sample (Figure 23), and a rather large concentration of montmorillonite in the bulk and <2-micrometer fractions (Figures 23, 24) set this sediment apart from the sediments encountered at previous sites.

A sample from the second core of Hole 108 does not match the sediment description of the shipboard scientists, and has a mineral composition resembling a hemipelagic mud. It may be a mislabeled sample which was submitted to our laboratory by mistake.

DISCUSSION AND CONCLUSIONS

The sediments of Site 98 are somewhat unusual, as only small quantities of quartz and very little feldspar were detected (Figures 1 and 2). These data and the observations by the shipboard palynologist, that there are no terrigenous pollen or spores in the sediments, suggest that there has been very little detrital material brought into this area.

Clinoptilolite is found in a number of cores on Leg 11. In Legs 8 and 9 in the equatorial Pacific (Cook and Zemmels, 1971a, b), clinoptilolite was usually associated with abundant volcanic detritus in various stages of alteration. In Leg 11, clinoptilolite occurs in sediments with apparently much less volcanic detritus.

In these sediments, perhaps most of the volcanic glass has been altered to clinoptilolite leaving very little evidence of its volcanic precursor. In Hole 105, clinoptilolite is abundant in Oligocene and Cretaceous sediments and forms the major constituent of a few thin beds. In these cases it probably represents ash beds that have been altered to clinoptilolite (see Site 105 in section on special samples below). In addition, a number of clinoptilolite-bearing samples are associated with chert (Hole 98, Cores 7 and 10; Hole 99A, Cores 8 and 9; Hole 105, Cores 12, 13, 16 and 19). This association was also observed by Hathaway and Sachs (1965). Clinoptilolite in association with palygorskite, as described by Bonatti and Joensuu (1968), is present in Cretaceous through Oligocene sediments (Hole 98, Cores 5 through 15; Hole 99A, Core 1; Hole 102, Core 14). Clinoptilolite occurs in Pleistocene and Pliocene sediments in Holes 99A and 103. Pleistocene and Holocene occurrences of clinoptilolite and other zeolites have been found in the Pacific, Atlantic, and Indian oceans. Their occurrences are summarized by Hay (1966).

Chlorite was observed in all upper Cenozoic sediments of Leg 11. The amount of chlorite in the bulk sample, as well as in the <2-micrometer fraction, commonly increases in the upper Cenozoic sediments (for example, Figures 11 and 12). Cooling climates in the source areas possibly resulted in less destruction of chlorite during soil formation as the Pleistocene approached. Thus, the younger sediments derived from these sources contain more chlorite than the older sediments.

Palygorskite is present at a number of locations, but it is most commonly found at Sites 98, 99 and 100 which are dominantly carbonate sections. At Site 98, palygorskite is absent in the youngest sediments and appears abruptly in Core 5 (Late Oligocene) accompanying a slight induration of the sediment and a simultaneous appearance of clinoptilolite. Palygorskite is found frequently in the Upper Jurassic sediments at Site 100, and is particularly abundant in the Oxfordian red clayey limestone. At Site 99A, however, palygorskite is restricted to the youngest sediment—a Pliocene-Pleistocene foraminiferal-nannoplankton ooze. In special samples studied by Hathaway in this report, it was observed that the palygorskite at Site 100 occurs as tiny fibers, about 1 micrometer in length, which are intimately intertwined with another mineral, possibly montmorillonite. Because palygorskite is relatively abundant in Leg 11, further work on these cores might be fruitful for those interested in studying the origin of palygorskite.

PART 2 (J. C. Hathaway)

A suite of special samples was collected on shipboard and analyzed separately from those reported above. Most of these special samples were either too small for

the analyses normally used by the Deep Sea Drilling Project, or they presented special problems of separation or preparation. I thank Anne Collins, Woods Hole Oceanographic Institution, who fractionated the samples, prepared the X-ray diffractometer mounts, and made the X-ray diffraction patterns and the punched tapes used in the analyses, and, Virginia Peters, Woods Hole Oceanographic Institution, who made the scanning electron micrographs. The punched tapes were analyzed by a computer program (Hathaway, in preparation); I checked the results by visual comparison with the diffractometer patterns.

The data for these samples are given in Table 11. Layer silicate minerals were differentiated only in selected samples from which a less than 2-micrometer fraction was taken. The proportions of the layer silicates shown are those in the <2-micrometer fraction. Only the total is given for the layer silicates in the bulk samples because diffraction lines for the layer silicates are often weak and ambiguous in diffraction patterns for randomly oriented powders. X-ray patterns of oriented aggregates of the concentrated clay-sized (<2-micrometers) fraction, made after treatment of the aggregates with ethylene glycol, and additional patterns made after heat treatment permit the distinction of the various layer silicates. However, in many samples the distribution of layer silicates is not the same in the clay-sized fraction as in the bulk sample. Tables 1 through 10 show that mica is relatively more abundant and montmorillonite less abundant in the bulk sample than in the clay-sized fraction. The proportions among the layer silicates shown in Table 11 should be compared only with the data for the less than 2-micrometer fraction in the preceding tables.

Results

Site 98

Samples were taken to confirm the presence of aragonite in the younger beds and to determine if magnesian calcite were present. The results show that aragonite decreases with depth, and that 8 per cent magnesian calcite containing 11 mol. per cent magnesite ($MgCO_3$) is present at a depth of about 4 meters, but except for a very small amount associated with a pyrite nodule, no magnesian calcite occurs below that depth.

Samples of cherts from Cores 7 (Eocene) and 10 (Paleocene) are composed predominantly of disordered cristobalite. Below the chert in Core 10, a zone of micritic chalk contains a slip surface at an angle of about 45 degrees which is coated with sepiolite in unusually large crystallites or aggregates of fibers all with the same optical orientation. The surface of the slip plane is also coated with dendritic manganese oxide. Figure 25 shows a photomicrograph and a

scanning electron micrograph of the sepiolite. The surrounding chalk contains a small amount of clinoptilolite (3 to 8 per cent). Hathaway and Sachs (1965) reported a similar association of sepiolite and clinoptilolite on the mid-Atlantic Ridge, but there the sepiolite occurred as very fine-grained massive material rather than large plates or aggregates of parallel fibers.

Site 99

Pieces of brown chert in Core 2 of Hole 99A consist of a relatively poorly crystallized quartz; the X-ray diffraction pattern is shown in Figure 26. The unconsolidated material in this core is of late Pliocene age, but the occurrence of the chert as broken pieces imbedded only in the bottom of Core 2 and similar composition for Hauterivian chert in Core 4 (Hole 99A), Tithonian chert in Core 10 (Hole 99A), and Tithonian-Kimmeridgian chert from Hole 100, Core 1 (Figure 26) suggests that the chert in Core 2 is actually older than late Pliocene. Although many cherts of Tertiary age are composed of disordered cristobalite and many cherts of Cretaceous and older age are composed of quartz, Core 4 of early Cretaceous age contains chert showing both disordered cristobalite and poorly crystallized quartz. The chert in Core 2, although obtained higher in the section and therefore a presumably younger sediment, contains no disordered cristobalite.

Considerable dolomite occurs in Cores 6 and 7. The dolomite shows displacements of diffraction lines corresponding to excess calcium carbonate ($CaCO_3$) in the amount of about 4 to 7 mol. per cent. Siderite in small amounts (2 to 3 per cent) occurs in Cores 2 and 7.

Barite was found in the core catcher sample of Core 6. This barite is probably a contaminant from the drilling mud used in this interval inasmuch as it is identical in particle size, shape, and roundness to the commercial barite that was used aboard the ship.

Site 100

Poorly crystallized quartz (Figure 26) occurs in chert of Tithonian-Kimmeridgian age in the core catcher sample of Core 1. The cherts of Oxfordian age in Cores 2 and 3 contain quartz of relatively normal crystallinity.

Palygorskite composes about 40 per cent of a sample from Core 5, Section 1 (261.15 meters depth). Examination with a scanning electronic microscope shows that the palygorskite consists of fibers less than 0.1 micrometers in diameter and about 1 micrometer in length. The fibers are intimately mixed with masses of thin crumpled flakes, probably montmorillonite.

The chilled margin of the basalt in Hole 100 shows considerable alteration. Montmorillonite is dominant,

TABLE 11 – Continued

Hole	Core	Section	Sampled at (cm)	Depth (m)	Composition, %														Distribution in <2µm Fraction				
					Calcite	Dolomite ^a	Siderite	Rhodochrosite	Quartz	K feldspar ^b	Plagioclase	Layer silicates undifferentiated ^c	Sepiolite	Palygorskite	Pyrite	Clinoptilolite	Phillipsite	Disordered cristobalite	Other	Kaolinite ^c	Mica ^c	Chlorite ^c	Montmorillonite ^c
102	1	1	5-6	0.05	28				14	1M	3	45							Aragonite 7	9	32	12	47
102	1	1	50-51	0.05	3				13		5	76											
102	1	2	113, black zone	2.63					8		6	86											
102	18	3	15-16	633.15	9				12	1M	5	70								9	28	3	61
102	18	3	19-20	633.19	16				18	1M	6	50								14	31	2	53
102	19	1	54, siderite	660.04	5	15(8.0)			3			20											
102	19	1	75	660.25	5				11	1M	8	73								14	16	4	66
103	1	1	27-28	0.27	15				20		15	50								8	34	8	50
103	1	1	77-78	0.78					21	2M	3	69											
103	1	1	145	1.45	9				21	2M	5	50								8	26	11	55
103	2	6	25-26	46.75	1	45(6.5)			15		5	33											
103	2	6	45-46	46.95		50(4.3)			15			35								16	25	3	56
103	3	6	73	102.23	20	7(9.9)			3			70								19	29		52
103	4	5	74-75	176.74					37	1M	6	50											
103	4	5	118-119	177.18					25	2M	7	52											
103	5	cc	hard lens	256.00	5	10(6.1)			5			9								25	25	5	57
104	1	1	3-4	0.30	65	2			8		5	20											
104	1	1	33-34 yellow	0.33	1				17	1(M)	7	75											
104	1	1	47-48 greenish black	0.47	?				19	1(M)	4	66											
104	1	1	73-74 pale green	0.73					34	1(M)	5	60											
104	1	1	77-78 olive yellow	0.77					12	2(M)	5	75											
104	1	1	95-97 olive yellow	0.95		tr(3.0)			12	4(M)	6	78											
104	1	1	108-109 olive brown	1.08	2	tr(3.3)			20	2(M)	8	65											
104	1	2	58-59 greenish black	2.08					12		6	70											
104	1	2	94-95 pale green	2.44					20	1(M)	5	63											
104	1	2	127-128 light yellow	2.77	35				10		10	40											
104	2	1	12	36.42	1	90(3.0)			1			8											
104	2	1	14	36.14	1	90(4.6)			1			5											
104	3	cc	sieve ret.	71.00					4														
104	10	1	41-42	615.91		93g(9.3)			2			5											
104	10	1	54-55	616.04		15g(14.3)			7	1(0) 4(M)		72											
105	1	cc		0.10	20				15	3	15	48											
105	2	cc		40.00	2				10	1	10	77											
105	3	cc		100.00					16		6	72											
105	3	cc		100.00					24		9	59											

TABLE 11 – Continued

Hole	Core	Section	Sampled at (cm)	Depth (m)	Composition, %													Distribution in <2 μ m Fraction					
					Calcite	Dolomite ^a	Siderite	Rhodo-chrosite	Quartz	K feldspar ^b	Plagioclase	Layer silicates undifferentiated ^c	Sepiolite	Palygorskite	Pyrite	Clinoptilolite	Phillipsite	Disordered cristobalite	Other	Kaolinite ^c	Mica ^c	Chlorite ^c	Montmorillonite ^c
106B	4	4	101	762.51			3				5(M) 1(O)	85					4	Gypsum trace					
106B	4	cc	nodule	763.00			90		2			8											
106B	5	6	bottom	944.00	3				15		9	70											
106B	7	1	50 HCl residue	1014.00					3			27					70						
106B	7	1	50	1014.00			70										10	Mangano-siderite	20				
106B	7	cc		1015.00					5			50					45						
108	1	cc		57.00	60				4		1	35											Amorphous material
108	4		drill collar	?	54				2		2	42											

^aExcess CaCO₃ in mol. % in dolomite structure shown in parentheses.

^b(M) = microcline; (O) = orthoclase; (S) = sanidine.

^cSelected samples were fractionated to obtain a clay-sized (<2 μ m) fraction. The proportions of the layer silicates, kaolinite, mica, chlorite and montmorillonite are shown at the right in percent of the total of these four minerals within the clay fraction.

^dPlus magnesian calcite (11 mol. % MgCO₃) – 8%.

^ePlus magnesian calcite (3 mol. % MgCO₃) – 4%.

^fPoorly crystallized quartz.

^gFerroan dolomite or ankerite; number in parentheses in mol. percent of FeCO₃ required to produce observed displacement of peaks.

^hHeulandite.

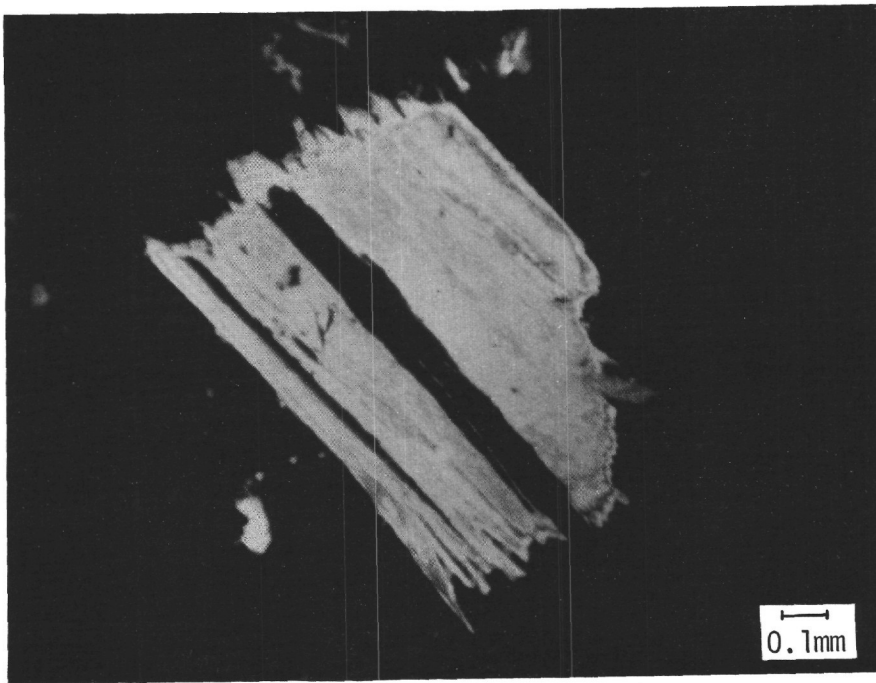
ⁱMagnesian calcite (4 mol. % MgCO₃).

^jMagnesian calcite (10 mol. % MgCO₃).

^kMagnesian calcite (10 mol. % MgCO₃).

^lMagnesian calcite (15 mol. % MgCO₃).

A



B

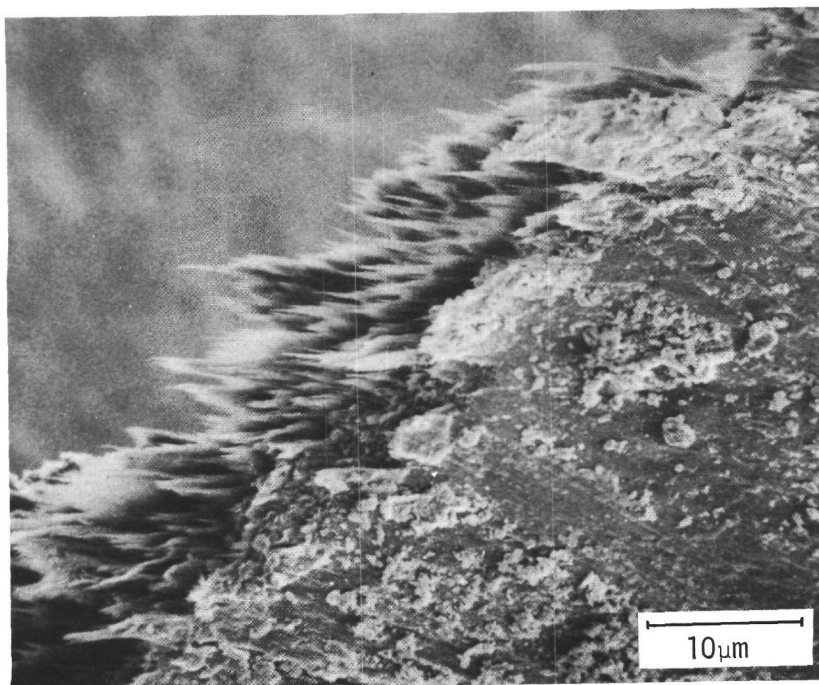


Figure 25. *Photomicrograph and scanning electron micrograph of sepiolite.*

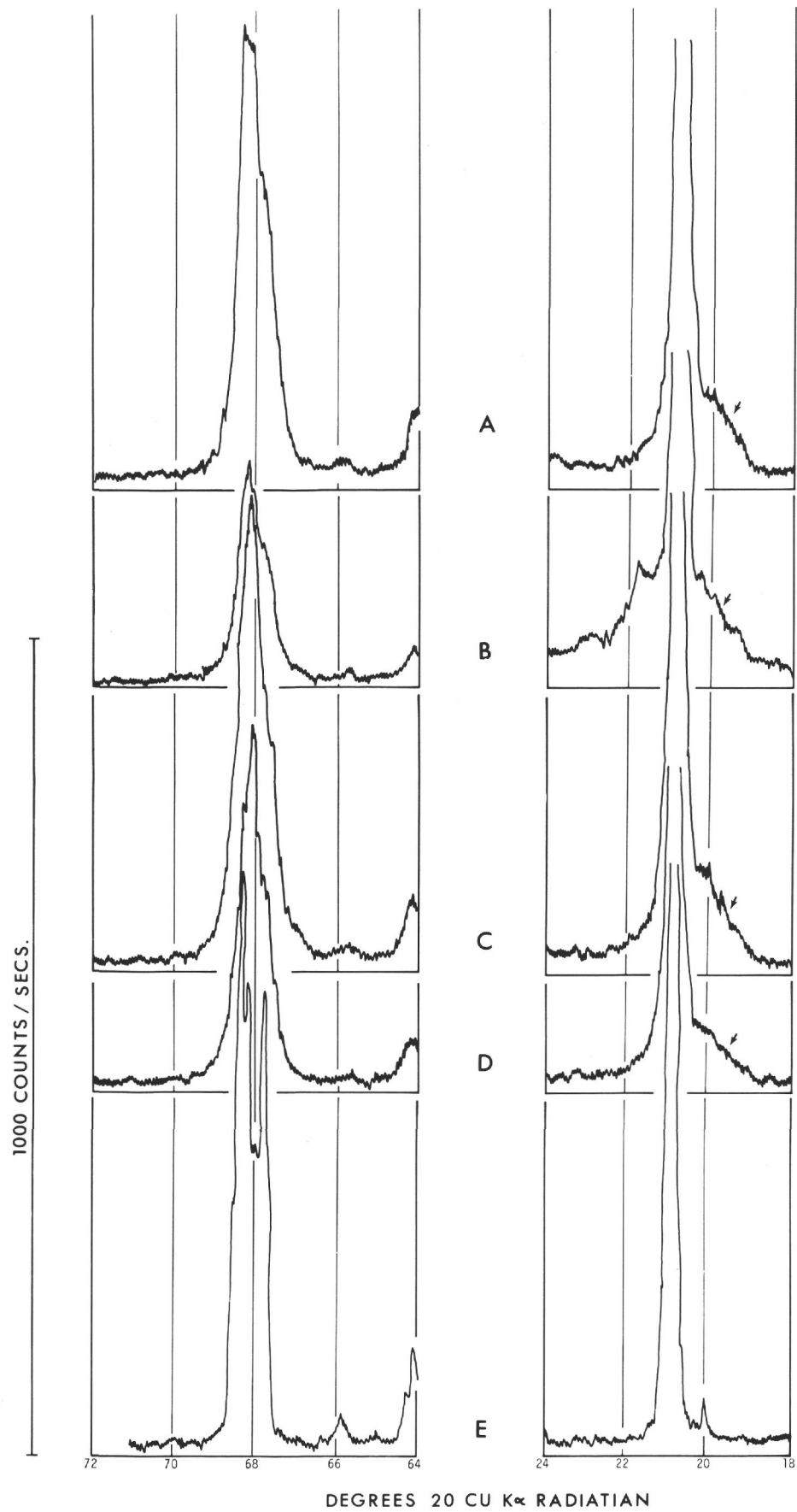


Figure 26. X-ray diffraction from poorly crystallized quartz samples.

but small amounts of kaolinite, mica and chlorite also occur. A peculiar, crumbly inclusion in the basalt (Core 12) is composed predominantly of calcite and quartz.

Site 101

A pyrite nodule in Core 1, Section 6 from Hole 101 contains a small amount of melanterite. This hydrated iron-sulphate may have formed by oxidation and hydration of the pyrite after collection of the sample.

Dolomite, siderite, manganosiderite and rhodochrosite occur in large amounts at various depth intervals in Hole 101A. Dolomite and siderite in substantial amounts occur together in a Middle Miocene sample from the base of Core 2. Some samples of Early Tithonian age from Core 10 contain as much as 45 per cent dolomite and small amounts of possible siderite. Rhodochrosite accompanies siderite in a sample of Albian age from Core 4. Siderite and manganosiderite occur in about equal amounts in a sample of Neocomian age from Core 6, Section 1. Manganosiderite and rhodochrosite occur together in a sample of Hauterivian age in Core 8.

If a trend truly exists, the samples (excluding those of Jurassic age) suggest that manganese is dominant in the earlier carbonates, and iron is dominant in the younger carbonates.

Channel samples of 4 centimeter average length were taken along the length of Core 10, Section 1 of Early Tithonian age to determine the range and variability of dolomite content in the section. Of the 20 channel samples and one spot sample, twelve contained dolomite; the amounts ranged from traces to 45 per cent with a mean of 16.0 per cent and standard deviation of 17.1 per cent. No correlation with other components (other than inverse closure-correlation with calcite) was observed. Considerable amorphous material occurs in the lower part of the section; it does not correlate with the dolomite, but with the absence of layer silicate minerals. Displacement of the diffraction maxima of the dolomite indicates the equivalent of 4 to 7 mol. per cent of excess calcium carbonate (CaCO_3) in the dolomite structure.

Site 102

Few special samples were analyzed from Site 102. The relatively high chlorite and mica content of the near surface sample of Core 1 suggests a northern source for the terrigenous detrital components of the sample (see Lancelot *et al.*, this volume; Hathaway, in press). Siderite is common in the samples from this site. One nodule of late Miocene age from Core 19 contains 57 per cent siderite and 15 per cent dolomite or possibly ankerite.

Site 103

Dolomite is abundant in samples of late Miocene age from Core 1, Section 6. This dolomite, like the examples described above, contains 4 to 7 mol. per cent excess calcium carbonate (CaCO_3) or its equivalent. A nodule from Core 3, Section 6 that was described as siderite aboard the ship, proved to contain dolomite rather than siderite. Diffraction peak displacement equivalent to 10 mol. per cent excess calcium and optical properties, which suggested the original identification as siderite, indicate that this sample probably contains ankerite rather than dolomite. A hard lens of Middle to Late Miocene age from Core 5 is composed dominantly of siderite. Apatite occurs in a sample of Late Miocene age from Core 4, Section 5.

Site 104

A hard, worm-burrowed, calcareous crust from the top of Core 1 is composed of 65 per cent calcite and 2 per cent dolomite; the rest is quartz, feldspar and layer silicates. The calcite does not show displacement of diffraction peaks that would identify it as a magnesian calcite. Cycles of dark green, pale green, and yellowish silty clays were sampled in Core 1 to determine if significant mineralogic assemblages accompany the various colors. Three to five per cent pyrite occurs in the dark green beds; pyrite was not detected by X-ray diffraction in the lighter-colored beds. Other than this, the different colored zones are not distinguished by any specific mineral assemblage. Siderite occurs in small amounts in most of the samples. Sediment of Late Middle Miocene age in Section 2 of Core 1 contains 6 to 8 per cent apatite. Bassanite (?) in Core 1 may have resulted from the partial dehydration of gypsum caused by oven drying during sample preparation.

Dolomite occurs in sediments of Late Middle Miocene age in Core 2 as hard, fine-grained, light bluish-gray rock that resembles lithographic limestone. The usual rhomb-shaped crystallites of dolomite are rare in this material, and its optical properties led to its identification aboard ship as limestone. Displacements of the X-ray diffraction peaks suggest the presence of 3 to 5 mol. per cent excess calcium carbonate (CaCO_3) in the structure.

Hard material of Early Miocene age from Core 10 was identified aboard ship as dolomitic siderite on the basis of its optical properties. X-ray analysis identifies it as ankerite (ferroan-dolomite) with peak displacements from normal dolomite indicating the equivalent of 9.3 mol. per cent FeCO_3 in the structure. When first recovered, this rock contained a considerable amount of gas—perhaps methane in the form of a clathrate—which formed bubbles on a wet, freshly-cut surface as the gas evaporated and escaped.

Site 105

The relatively complete section obtained from Hole 105 permitted an extensive set of special samples to be collected. Most of these samples were fractionated for study of the less than 2-micrometer fraction, and although the points of sampling do not necessarily correspond to those represented in Tables 1 through 10, they do tend to bracket one another and provide an indication of the agreement of trends between the two sets of data. Figure 27 shows the ratio of chlorite plus mica to the total of chlorite, mica, kaolinite and montmorillonite. In most samples kaolinite is minor, and chlorite is limited largely to the top four cores and the lowest four cores. Therefore, the ratio is influenced primarily by mica and montmorillonite.

Agreement is good over large parts of the section. The wide scatter of points for Cores 5 through 9 is the result of the special sampling of thin layers and of unusual areas in the multicolored zone, whereas, the routine samples are usually composites of representative beds. The reason for the wide variation of values between the two sets of samples in Cores 34 through 40 is not known. A trend showing more chlorite and mica in the sediment of Oxfordian age than in the overlying sediments of Kimmeridgian and Tithonian age is evident in both sets of data. The distinct increase in mica and chlorite from the sediments of Late Pliocene age (Core 3) to those of Pleistocene and Holocene age (Cores 2 and 1) is also evident. This same trend occurs at the other sites (see Lancelot *et al.*, this volume).

Dolomite is rare in the samples from Hole 105. It occurs in only one of the samples (Core 2) shown in Table 8, and it occurs in none of the samples from Hole 105 shown in Table 11. Siderite was found in several samples; one, of Albian age, contains 65 per cent siderite and 30 per cent manganosiderite (?) (105-13, cc, siderite, 331.00 meters depth). Rhodochrosite occurs as small pellets in upper or middle Miocene sediments in Core 4, Section 3. Micrographs of these pellets are shown by Lancelot *et al.*, (this volume).

Quartz occurs principally as detrital grains, presumably terrigenous. Only one sample of chert was recovered from Hole 105. This chert consists of chalcedonic quartz cementing plates of the planktonic crinoid *Saccocoma* in Core 34, Section 3 (not represented in Table 11). The disordered cristobalite found in Cores 12 to 22 (Table 11) does not form chert, but occurs as small spherules or irregular particles disseminated through unconsolidated sediment.

Feldspars, mainly plagioclase and very small amounts of microcline, make up no more than a few per cent of most samples from Hole 105. Exceptions are: the

Pleistocene samples from the first two cores which contain as much as 18 per cent terrigenous detrital feldspar; a sample of basalt; and, the palagonite-rich samples from just above the basalt in Core 40, which contain as much as 25 per cent potassium feldspar. The X-ray diffraction characteristics (Figure 28) of this feldspar meet the criteria for high sanidine given by Wright (1968). The sanidine occurs in shard-shaped masses or linings of cavities in a matrix of montmorillonite. Figure 29 shows a crystal growth pattern that strongly suggest authigenic origin (see also Lancelot *et al.*, this volume).

Clinoptilolite is a prominent constituent of samples from Cores 9 through 23. Its greatest concentration, 70 per cent, occurs in a silt band in the core catcher sample of Core 13. A photomicrograph of clinoptilolite from this core is given in Lancelot *et al.*, (this volume). The occurrence of clinoptilolite in such silty bands and its localization in certain zones of the section suggest that it is an alteration product of volcanic ash. Although beds of ash composed of glass shards were not observed, one white bentonite-like band composed almost entirely of montmorillonite and disordered cristobalite occurs in this zone (Sample 105-12, cc, white clay). It is unlikely that this bed originated in any other way but by the alteration of volcanic material. The similarity of the bands of clinoptilolite to this bed and the common occurrence of clinoptilolite in volcanic tuffs (Hathaway and Sachs, 1965) support an ultimate origin as volcanic detritus. Alteration to montmorillonite, cristobalite, zeolites, or persistence as volcanic glass must depend largely on the composition of the original ash rather than the environment of deposition.

Another zone of clinoptilolite occurs in Core 5. One sample contains phillipsite and a zeolite with the thermal characteristics of heulandite. A small amount of phillipsite also occurs in Core 14.

The multicolored zone of Cores 5 through 9 contains much goethite, a manganese oxide with the structure of goethite (groutite?), and some manganese nodules composed of todorokite. Another characteristic of the multicolored zone is the relatively large concentration of kaolinite in the clay fraction. Concentrations of 20 per cent to 25 per cent are unmatched in any other zone from Hole 105.

Sphalerite occurs at the base of the multicolored zone. The largest concentration is in Core 9, Section 3 in a silty zone resembling a burrow filling. Pyrite is also prominent in the sample. (See Lancelot *et al.*, this volume, for a photomicrograph of this sphalerite and pyrite, and for a discussion of the possible origin of the multicolored zone.)

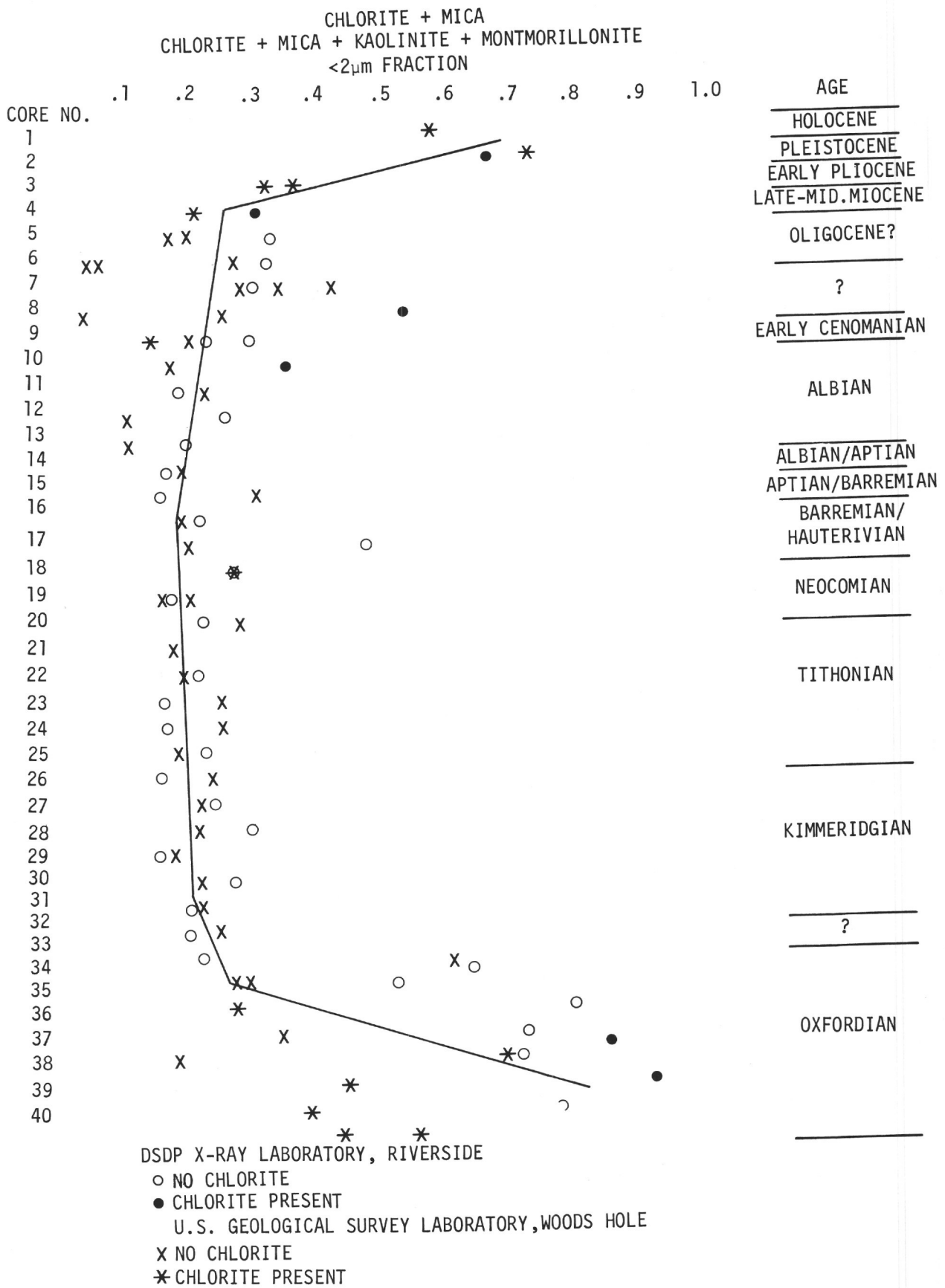


Figure 27. Graph showing the ratio of chlorite plus mica to the sum of chlorite mica, kaolinite, and montmorillonite.

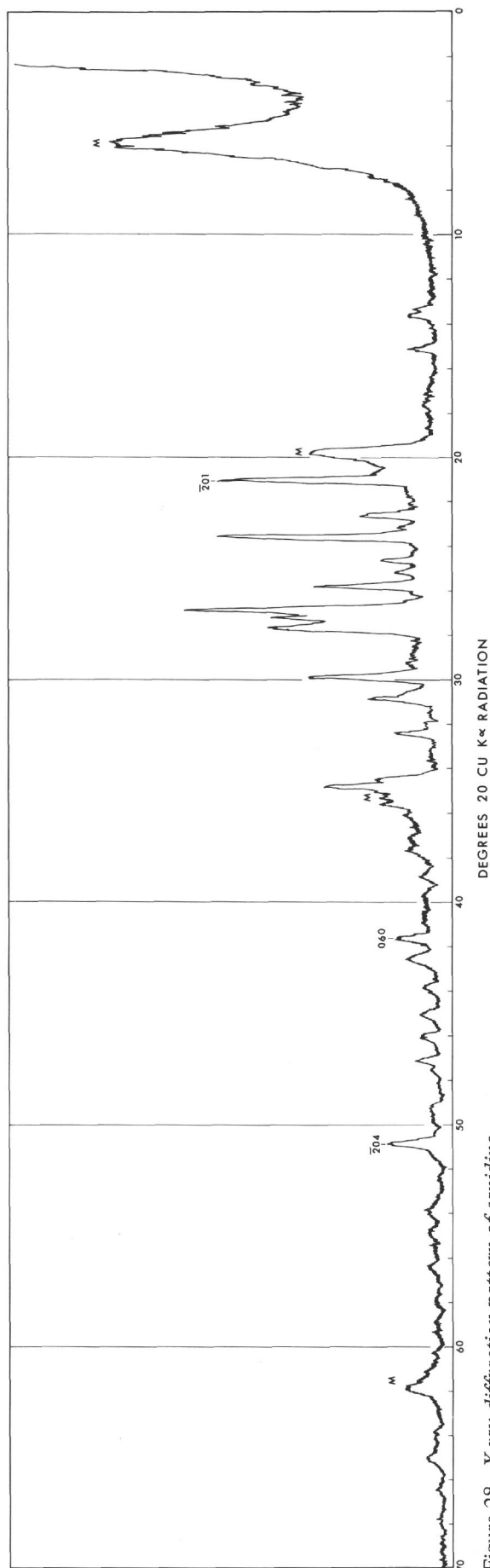


Figure 28. X-ray diffraction pattern of sanidine.

Barite occurs as clear wafer-shaped crystals as large as 5 centimeters in diameter and 2 centimeters thick imbedded in pale reddish-brown limestone in Core 33, Section 5. The barite is clearly not contamination, but appears to be an authigenic growth in the sediment.

Native copper in tiny (1 millimeter in diameter) crystals imbedded in a thin layer of palagonitic material occurs in a thin veinlike band cutting diagonally through Core 38, Section 2. Such materials, about 20 meters above the contact of the sediments with the basalt, indicate that hydrothermal or magmatic activity occurred in the region about 1.5 million years after the deposition of the sediments in contact with the basalt.

Magnesian calcite (4 to 15 mol. per cent $MgCO_3$) occurs in baked limestone just above the basalt in Core 40. The magnesium was probably introduced during contact metamorphism of the limestone. It is noteworthy that the calcite associated with the vein bearing the native copper has a similar magnesium-carbonate content.

Site 106

Only six samples were analyzed from Hole 106B. These samples were selected principally to confirm the presence of siderite in nodules that were recovered. One nodule from Core 7 contains 20 per cent manganosiderite as well as siderite. This zone also contains considerable concentrations of disordered cristobalite.

Site 107

No samples were collected from Site 107.

Site 108

Two samples were collected from Hole 108. The amorphous material noted in Table 11 is composed of siliceous fossils, chiefly radiolarians and sponge spicules.

Summary

The minerals found in the study of these special samples and the maximum amounts of each mineral are given in Table 12. The samples contain at least 33 minerals detectable by X-ray diffraction. Some minerals unusual in marine sediments and some unusually large concentrations of more common minerals were found. Among these are: ankerite, 93 per cent; barite, 100 per cent; bassanite (?); native copper, 100 per cent; dolomite, 90 per cent; groutite (?); manganosiderite, 46 per cent; melanterite, 10 per cent; palygorskite, 40 per cent; rhodochrosite, 65 per cent; sanidine, 25 per cent; sepiolite, 95 per cent; siderite, 90 per cent; and, sphalerite, 55 per cent.

TABLE 12
Samples Containing Maximum Amounts of Various Minerals

Mineral	Amount in Per cent	Samples Containing This Amount				Interval or Description	Depth Below Bottom (m)
		Hole	Core	Section			
Amphibole	5	106	2	1	124-126 cm	46.25	
Ankerite	93	104	10	1	41-42 cm	615.91	
Apatite	9	103	4	5	118-119 cm	117.18	
Aragonite	75	98	1	1	33-33.5 cm	0.34	
Barite	100	105	33	5	95 cm	564.95	
Bassanite(?) ^a	?	104	1	1	47-48 cm	0.47	
Calcite	100	98	13	cc		281.00	
Chlorite	12	105	2	cc		40.00	
Clinoptilolite	70	105	13	cc	silt layers	331.00	
Copper, native	100	105	38	2	106 cm	605.56	
Cristobalite, disordered	73	98	10	1	68-71 cm	222.68	
Dolomite ^b	90	104	2	1	12 cm	36.12	
Goethite	60	105	9	3	43 cm	289.43	
Groutite(?)	65(?)	105	5	1	84 cm	246.34	
Gypsum	3	98	11	2	composite	232.31-233.75	
Hematite	5	101A	6	1	70 cm	388.20	
Heulandite	10	105	5	2	154 cm	248.54	
Kaolinite	18	105	6	cc		259.00	
Magnesian calcite ^c	25	105	38	2	124 cm	605.74	
Manganosiderite	46	101A	6	1	76 cm	388.26	
Melanterite ^a	10	101	1	6	pyrite	41.00	
Mica	68	101A	6	1	26-28 cm	681.26	
Montmorillonite	95	105	37	5	33 cm, green mat.	600.33	
Quartz, poorly crystalized	100	99A	2	cc		24.00	
Palygorskite	40	100	5	1	133-134 cm	261.15	
Phillipsite	15	105	5	2	154 cm	248.54	
Pyrite	85	101	1	6	pyrite	41.00	
Rhodochrosite	65	101A	8	cc	soft material	543.00	
Sanidine	25	105	40	1	77-78 cm	621.77	
Sepiolite	95	98	10	1	128-129 cm	223.28	
Siderite	90	106B	4	cc	nodule	763.00	
Sphalerite	55	105	9	3	117 cm	290.17	
Todorokite	10	105	7	cc	Mn nodule, upper part	268.80	

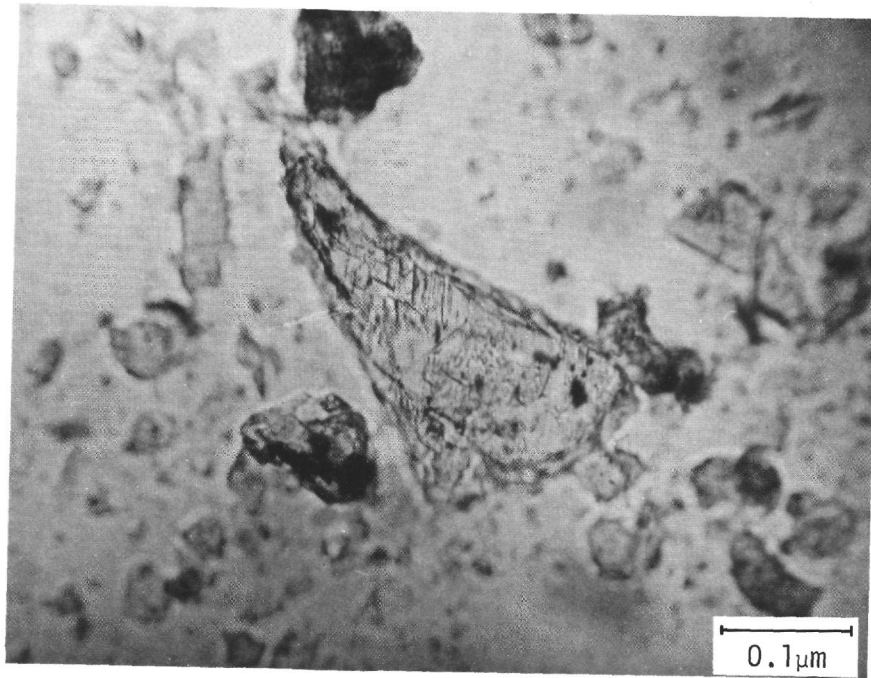
^aMay be an artifact produced by partial dehydration of gypsum during sample preparation.

^bX-ray diffraction peaks displaced an amount equivalent to 3 mol. percent excess CaCO₃.

^c10.0 mol. percent MgCO₃.

^dMay have developed after collection of sample by oxidation and hydration of pyrite.

A



B



Figure 29. *Photomicrograph and scanning electron micrograph of sanidine.*

Some common minerals occur in unusual forms. Quartz similar to chalcedony shows some unusual X-ray diffraction peak breadth effects. Disordered cristobalite occurs in tiny spherules disseminated in the sediment. Sepiolite is present in unusually large crystallites and aggregates of parallel fibers. Magnesian calcite was found in Jurassic sediments altered by contact metamorphism. Clinoptilolite occurs in interpenetrating and twinned crystals, and sanidine occurs in delicate authigenic growths that fill cavities in palagonitic material.

Agreement is good between the sets of data obtained independently by the authors.

REFERENCES

- Biscaye, P. E., 1965. Mineralogy and sedimentation of Recent deep-sea clay in the Atlantic Ocean and adjacent seas and oceans. *Bull. Geol. Soc. Am.* **76**, 803.
- Bonatti, E. and Joensuu, O., 1968. Palygorskite from Atlantic deep sea sediments. *Am. Mineralogist.* **53**, 975.
- Cook, H. E. and Zemmels, I., 1971. X-ray mineralogy studies-Leg 8. In Tracey, J. I. et al., 1971a. *Initial Reports of the Deep Sea Drilling Project, Volume VIII*. Washington (U.S. Government Printing Office), in press.
- _____, 1971b. X-ray mineralogy studies-Leg 9. In Hays, J. D. et al., 1971, *Initial Reports of the Deep Sea Drilling Project, Volume IX*. Washington (U.S. Government Printing Office), in press.
- Ericson, D. B., Ewing, M., Wollin, G. and Heezen, B. C., 1961. Atlantic deep-sea sediment cores. *Bull. Geol. Soc. Am.* **72**, 193.
- Hathaway, J. C. and Sachs, P. L., 1965. Sepiolite and clinoptilolite from the mid-Atlantic Ridge. *Am. Mineralogist.* **50**, 852.
- Hathaway, J. C., in press, Regional clay-mineral facies in the estuaries and continental margin of the United States East Coast. *Geol. Soc. Am. Memoir* **133**.
- Hay, R. L., 1966. Zeolites and zeolitic reactions in Sedimentary rocks. *Geol. Soc. Am. Special Paper* **85**.
- Wright, T. L., 1968. X-ray and optical study of Alkali Feldspar: II. An X-ray method for determining the composition and structural state from measurement of 2θ values for three reflections. *Am. Mineralogist.* **53**, 88.